# Energy Management and Smart Charging of PEVs in Isolated Microgrids

by

Talal Alharbi

A thesis
presented to the University of Waterloo
in fulfillment of the
thesis requirement for the degree of
Master of Applied Science
in
Electrical and Computer Engineering

Waterloo, Ontario, Canada, 2015

## Author's Declaration

I hereby declare that I am the sole author of this thesis. This is a true copy of the thesis, including any required final revisions, as accepted by my examiners.

I understand that my thesis may be made electronically available to the public.

## Abstract

Microgrids are defined as a cluster of loads and micro-resources operating as a single controllable entity that provides both power and heat to its local area. Typically, these rely on conventional diesel generators, but with recent developments are expected to include more renewable energy sources (RESs), battery energy storage systems (BESSs), and plug-in electric vehicles (PEVs). Both RESs, such as wind and solar, and PEVs can reduce greenhouse gas (GHG) emissions significantly such as carbon dioxide ($CO_2$) which are released from burning fuel by generators or conventional vehicles.

Energy management in isolated microgrids is an important task since these have limited generation capacity and are expected to rely on various uncontrollable resources to match and balance the demand-supply gap. Moreover, PEVs present a promising solution to GHG emissions but on the other hand, their increased penetration can impact power system operation, particularly so in isolated microgrids. Therefore, PEV load management is considered to be a crucial issue. Similarly, demand response (DR) has the potential to provide significant flexibility in operation of isolated microgrids with limited generation capacity, by altering the demand and introducing an elasticity effect.

The present research work examines the impact of uncontrolled and controlled (smart) charging of PEVs using a comprehensive mathematical optimization model for short-term operation of the isolated microgrid. This model determines optimal energy management solutions combining generation from different resources such as diesel generators, wind turbines, solar panels, and BESSs, and incorporates the DR options as well.

Furthermore, the thesis presents a stochastic optimization model after creating several probabilistic operational scenarios for energy management and smart charging of PEVs in short-term operation of the isolated microgrid considering fixed and optimal DR options. The proposed stochastic optimization model studies the impact of wind and solar generation output variability as well as the effect of uncertain energy consumption patterns of customers; and also the stochastic nature of the state of charge (SOC) of the PEV battery at the start of charging.

Several case and scenario studies considering a modified CIGRE isolated microgrid benchmark test system, and using the proposed models are presented and evaluated, to obtain insights into the effect of smart charging *vis-à-vis* uncoordinated charging accompanied by DR options in overall energy management of the isolated microgrid.

**Acknowledgements**

All praise and thanks are due to Allah alone, the Exalted, the Most Merciful, and the Most Giving for all His blessings that He bestowed upon me. May Allah accept my humble efforts, and be pleased with me.

I would like to express my deepest and sincere gratitude and appreciation to my supervisor, Professor Kankar Bhattacharya for his invaluable support, continuous guidance, and encouragement throughout the course of my MASc studies at the University of Waterloo. It has been an honor and privilege to have completed my research under his supervision.

I would like also to greatly thank and appreciate Professor Magdy Salama and Professor Ramadan El-Shatshat for serving as members of my thesis committee. Their efforts, valuable comments, and support in reviewing this thesis are highly appreciated.

Further, I am thankful to the Saudi Arabian Ministry of Higher Education represented by Qassim University for their financial support. My appreciation and thanks are also extended to the Saudi Arabian Culture Bureau in Canada for their continuous assistance throughout the course of my studies at the University of Waterloo.

I wish to express my sincere thanks to my wonderful mother, Norah, and my bothers and sisters for believing in me, praying for me, and supporting my academic career although it meant being away from them.

Special thanks are extended to my friends: Omar Alrumayh, Walied Alharbi, Abdulaziz Almutairi, Abdullah & Omar Bin Humayd, Omar Hafez, Badr Lami, Hisham Alharbi, and Nizar Alsharif for their sincerity, support, and encouragement during my academic journey. Also, I will not forget Rayed Al-Yousef, Hesham Abduljabbar, and Omar Alghamdi.

Last but not least, I would like to thank all my friends in Waterloo, who have enriched my life and made it enjoyable.

## Dedication

To the soul of my Father

To my wonderful mother, **Norah**

for her endless love and measureless support & prayers

# Table of Contents

# List of Tables

# List of Figures

# Nomenclature

## *Indices*

| | |
|---|---|
| $t$ | Index of time interval, hours, $t = 1, 2, ..., T$ |
| $i, j$ | Index of bus number |
| $ev$ | Index of buses where EVs are located |
| $N$ | Index of total number of buses |
| $M$ | The end hour of the PEV charging period |
| $s$ | Index of scenario, $\mathrm{s} \in \mathrm{S}$ |
| $up$ | Demand variation upward |
| $dn$ | Demand variation downward |
| $unmet$ | Unmet energy |
| $ch, dis$ | Charging and discharging |

## *Parameters*

| | |
|---|---|
| $G_{ij}, B_{ij}$ | Conductance and admittance of feeder $i$-$j$, $[pu]$ |
| $a_i, b_i, c_i$ | Cost parameters for each diesel generator |
| $Co_t^{DR}$ | Incentive paid by the MGO to customers for DR, $[\$/\,kW]$ |
| $Co_t^{unmet}$ | Cost for unmet energy, $[\$/\,kWh]$ |
| $Co_t^{PEV}$ | Transaction cost for charging the PEV, $[\$/\,kWh]$ |
| $PDC_t$ | Maximum allowable peak demand, $[kW]$ |
| $P_{max}^{BESS}$ | Maximum power allowed to charge or discharge the BESS, $[kW]$ |
| $P_{max}^{PEV}$ | Maximum power allowed to charge the PEVs, $[kW]$ |
| $\eta^{out}, \eta^{in}$ | Discharging and charging efficiency of the BESS, $[\%]$ |
| $E_{min}^{BESS}, E_{max}^{BESS}$ | Minimum and Maximum allowable energy stored in the BESS, $[kWh]$ |
| $E_{min}^{PEV}, E_{max}^{PEV}$ | Minimum and Maximum allowable energy stored in the PEV, $[kWh]$ |

| | |
|---|---|
| $B_{dn}, B_{up}$ | % of maximum demand variation downward and upward |
| $V_{max}, V_{min}$ | Maximum and Minimum voltage limits $[pu]$ |
| $e^{a}$ | Forecasting error factor of each state |
| $\rho^{s}$ | Probability of each scenario |
| $Pd_{i,t}$ | Microgrid's active power demand at each bus and hour, $[kW]$ |
| $Qd_{i,t}$ | Microgrid's reactive power demand at each bus and hour, $[kVAR]$ |
| $PW_{i,t}$ | Forecasted wind turbine power generation at each bus and hour, $[kW]$ |
| $PV_{i,t}$ | Forecasted solar power generation at each bus and hour, $[kW]$ |
| $Pg_{min}, Pg_{max}$ | Minimum and maximum active power generation of each unit, $[kW]$ |
| $Qg_{min}, Qg_{max}$ | Minimum and maximum reactive power generation of each unit, $[kVAr]$ |

## *Variables*

| | |
|---|---|
| $P^{BESS,dis}_{i,t}$ | BESS power during discharge phase at each bus and hour, $[kW]$ |
| $P^{BESS,ch}_{i,t}$ | BESS power during charging phase at each bus and hour, $[kW]$ |
| $X^{ch}_{i,t}$ | BESS binary charging decision $[1 = Charging; 0 = Otherwise]$ |
| $X^{dis}_{i,t}$ | BESS binary discharging decision $[1 = Discharging; 0 = Otherwise]$ |
| $E^{BESS}_{i,t}$ | Available Energy stored of BESS at each bus and hour, $[kWh]$ |
| $E^{PEV}_{ev,t}$ | Available Energy stored of PEV battery at each bus and hour, $[kWh]$ |
| $P^{PEV}_{ev,t}$ | PEV charging power located at the residential area *ev* at hour *t*, $[kW]$ |
| $Pg_{i,t}$ | Active power generation at bus i and hour t, $[kW]$ |
| $Qg_{i,t}$ | Reactive power generation at bus i and hour t, $[kVAr]$ |
| $dP_{i,t}$ | Variable demand when DR is applied, $[kW]$ |
| $dVar^{dn}_{i,t}$ | Demand variation downward when DR is applied, $[kW]$ |
| $dVar^{up}_{i,t}$ | Demand variation upward when DR is applied, $[kW]$ |
| $B_{dn}, B_{up}$ | % of maximum demand variation downward and upward |
| $P^{unmet}_{i,t}$ | Unmet load at each bus and hour, $[kW]$ |

# Glossary of Terms

| | |
|---|---|
| GHG | Greenhouse gas |
| IEA | International Energy Agency |
| RES | Renewable Energy Sources |
| EVs | Electric Vehicles |
| PEVs | Plug-in Electric Vehicles |
| DGs | Distributed Generators |
| OPF | Optimal Power Flow |
| G2V | Grid to Vehicles |
| V2G | Vehicles to Grid |
| AMIs | Advanced Metering Infrastructures |
| PHEVs | Plug-in Hybrid Electric Vehicles |
| TOU | Time-of-Use |
| PV | Photovoltaic |
| DR | Demand Response |
| ESSs | Energy Storage Systems |
| MINLP | Mixed Integer Nonlinear Programming |
| NLP | Nonlinear Programming |
| MGO | Microgrid Operator |
| DSM | Demand Side Management |
| BESSs | Battery Energy Storage Systems |
| SOC | State of Charge |
| DSM | Demand Side Management |
| GAMS | General Algebraic Modeling System |

# Chapter 1

# Introduction

## 1.1 Motivation

In the recent years, concerns associated with the reliability and efficiency of classic power system networks and environmental issues that cause climate change, have led power system networks to undergo substantial transformations. Penetration of renewable energy sources (RESs) has been rising at a rapid rate due to economic and political reasons. Based on a report by the International Energy Agency (IEA), by 2035 the renewable resources will account for 31% of the world's total energy generation. In Canada and particularly in Ontario, hydro, wind, and solar are the three major renewable resources that are expected to contribute a major share of the total supply [1].

Moreover, in order to reduce greenhouse gas (GHG) emissions, electricity customers have been participating in various ways. Under the umbrella of demand side management (DSM), demand response (DR) is one, wherein, electricity customers can participate in reducing GHG emissions and enhancing the performance of the electrical grid by reducing the peak demand. Also, with the use of electric vehicles (EVs) and their penetration level is increasing, can have a significant impact on reducing GHG. According to the World Wide Fund for Nature (WWF)-Canada, having 12,000 EVs on the road each year would result in the reduction of 6.7 mega tonnes of carbon dioxide ($CO_2$) emissions by 2025 [2].

The system operations are no longer centralized because of the two-way flow of electricity and information, which has paved the way to characterize the grid as a "smart grid ". The smart grid basically incorporates RESs, energy storage systems, DSM strategies, and EVs in a system that has two-way communication infrastructure, smart meters, *etc.* [3].

The microgrid is defined as a cluster of loads and micro-resources operating as a single controllable entity that provides both power and heat to a local area. Microgrids typically have two modes of operation: grid-connected or isolated mode. The decentralized system operation adopted in a microgrid can both impose challenges and offer solutions.

The increased penetration of plug-in electric vehicles (PEVs) in a distribution system has various negative impacts on the grid in terms of system load, power losses, power quality, and overload conditions [4–6]. Isolated microgrids have limited generation capacity, and introducing new loads such as charging PEVs might lead to a demand-supply balance problem and consequently blackouts or load shedding. Uncontrolled charging of PEVs would put the system in a critical situation, while smart charging of PEVs is advantageous for both customers and microgrid operators (MGO) [5].

DR strategies, which are defined as changes in electrical usage by demand side sources in response to changes in price or certain incentives, have the ability to boost system reliability by modifying load profiles and reducing the peak demand. This can also help the MGO to meet demand-supply constraints [7,8]. Many benefits can be accrued by both customers and MGOs by using DR schemes in microgrids. However, it is important to consider the uncertainty associated with wind speed, solar insolation, and forecasted demand, which is a challenging task in isolated microgrids.

In view of the above, developing an appropriate scheduling model that coordinates the charging of PEVs and manages the controllable and uncontrollable resources in isolated microgrids is the main motivation of this research. The energy management strategy is intended to ensure coordination between diesel generator units, wind turbines, solar panels, and battery energy storage to achieve economic and efficient operation. As well, the impact of uncertainties on the operation of the system is needed be examined within the mathematical model framework.

## 1.2 Literature Review

In past few years, the penetration of distributed generators (DGs), both diesel and renewable based, have grown remarkably as also that for energy storage devices.

Jiang *et al.* [9] studied the energy management of a microgrid in both grid-connected and islanded modes. A double-layer coordinated control for microgrid management consisting of a schedule layer and a dispatch layer are proposed to deal with the uncertainties between forecasted and real-time data. The schedule layer acquires the economic operation of the forecasted data, while the dispatch layer supplies power based on real-time data to optimize the power flow and regulate voltage. An optimal power flow (OPF) problem for a microgrid system is proposed [10] to investigate energy management scheduling while effectively using a battery storage system after integrating wind energy sources. In [11], the economic load dispatch problem to optimize the fuel cost during the grid-connected operation mode while guaranteeing stable operation in the isolated operation mode of a multi-microgrid is examined. The proposed DSM algorithm utilized fixed and adjustable droop control so that DGs was to ensure a balance between demand and supply, according to the power-frequency ($f$ - $p$) droop characteristics.

The benefits that comes from driving EVs are significant, such as lowering the fuel costs of the vehicles and mitigating emissions. Therefore, the interaction between driving EVs and the electric network system has to be studied carefully. The potential impact of PEV charging on distribution and microgrid systems has been reported in the literature. There are two main scenarios to charge PEVs, uncontrolled charging and controlled (smart) charging [4,12–14]. Accommodating PEVs and relying only on uncontrolled charging has been found to be detrimental to electric power system equipment, such as transformer insulation lifetime and reliability [12, 14, 15]. As a result, utilities are left with two solutions to avoid negative and undesirable impacts; either by upgrading the electric power system infrastructure, such as installing new generation units to meet the excess power demand or by coordinating PEV charging [4, 12–15]. The coordination of PEV charging is mainly categorized into two possible approaches: centralized and decentralized [16]. The centralized approach is based on the availability of advanced metering infrastructure (AMI) that has the capability for two-way communication. On the other hand, the decentralized approach primarily relies on broadcasted signals, for instance, pricing information, sent to the vehicle owner to achieve a local decision without guaranteeing an action [16].

In [4], the impact of uncoordinated plug-in hybrid electric vehicles (PHEVs) charging on a residential distribution system has been investigated to optimize the power losses and the grid load factor with consideration of deterministic and stochastic load profiles. The results illustrated that uncoordinated charging of PHEVs could lead to a new demand peak, which causes grid problems.

The hourly integration, coordination, and operation of volatile wind power generation and EVs in power systems was studied in [13] by a stochastic security constrained unit commitment model. The objective was set to minimize the expected grid operation cost while considering the random behavior of large penetration of PEVs as mobile distributed loads and storage devices at the same time. The concepts of grid to vehicles (G2V) and vehicles to grid (V2G) were studied. When PEVs are connected to the grid, they will draw energy and store it in their batteries, and are capable of injecting the energy back to the grid at different times and locations to reduce grid operation costs and losses.

Sortomme *et al.* [12] carried out a study of coordinated charging of different penetration of PHEVs to minimize distribution system losses and load variance, maximize load factor in a balanced radial distribution system. The study showed that applying load factor or load variance as the objective function instead of system losses would solve the convexity problem and decrease the computation burden.

Industrial microgrids are gradually taking shape in many countries. Derakhshandeh *et al.* [14] proposed a dynamic OPF formulation to schedule the flow of energy in industrial microgrids. PV generation panels coupled with storage system, PEV charging loads, and generators including combined heat and power (CHP) units were coordinated, and the flow of energy was intelligently managed while considering all the related constraints. The intermittent nature of renewable energy and randomness in the load profile were not considered in this work.

In [17], the problem of coordination between wind and PEVs in a microgrid to optimize energy dispatch is examined, and deterministic and stochastic scenarios of wind power are presented. In order to balance generation and demand while meeting the PEV requirements, three coordinated energy dispatch methods are proposed, which are: valley searching, interruptible, and variable-rate dispatching. The variable-rate dispatching method was better in utilizing more wind energy during the night, mitigating the energy drawing from the grid during the day, and receiving a high degree of satisfaction regarding to the vehicles owners.

A study in [18] proposes a charging method for EVs to minimize the cost of charging and realize peak clipping and valley filling. The proposed method was utilized to control and adjust EV charging power and time in response to Time-of-Use (TOU) price in a regulated market. As a result, mitigating the peak demand and filling the valley in the demand profile were achieved.

In [19], an estimation of distribution algorithm (EDA) is used to allocate electric energy of the PHEVs connected to the grid and hence maximize the average battery state of charge (SOC) level for all PEVs. A probabilistic modeling for various variables such as parking time and initial SOC were considered.

The integration between EVs and DR with customer choice in a large power system network was investigated in [20]. An approach to manage home area networks is proposed that permits customers to control their own demand based on comfort indices. The study showed that maintaining the original peak demand with a large EV penetration could lead to consumer inconvenience. As a result, utilities have to address this problem by either installing DGs or upgrading their equipment to accommodate high EV penetration in their electric power network.

As the line losses are proportional to the current squared, a network with low demand would be more energy efficient. Thus, a reduction in the load would increase the efficiency of the system while decreasing the peak demand. Hence, DSM plays a vital role in progressing forward an efficient network. One of the predominant DSM programs is DR. For the most part, DR, which is classified into two types that direct and indirect programs, is carried out by either utility companies' decisions or customers' choices. DR strategies have the ability to boost system reliability by modifying the load profile, such as reducing peak demand and shifting energy consumption to different periods. This can help the MGO to meet demand-supply constraints [7,8]. Many benefits can be accrued by both customers and the MGO by using DR in microgrids.

In this section, a review of some of the current research work on DR is presented.

Dietrich *et al.* [7] proposed two different DR techniques in an isolated system with high wind integration: demand shifting and peak shaving. The peak shaving approach is cost based, while demand shifting depends upon elasticity. The objective in [7] is to minimize the total cost considering the two DR approaches. The authors conclude that DR programs can have savings up to 30% of the total cost, depending on wind variation. Though [7] studied the operation of a microgrid in the presence of high wind integration and participant of DR, neither PVs nor battery energy storage systems (BESSs) and PEVs were included.

A multi-agent approach was proposed in [21] to form an intelligent energy management system in microgrids while utilizing DR and distributed energy storage systems in order to mitigate the peak demand and decrease the cost of electricity to customers. An index of customers' priorities of load and appliances were included in this study which concluded that customers with a high-priority index receive energy at a lower cost when they participate in DR.

In Canada, many remote communities are located off-grid and operated as isolated microgrids supplied mostly from diesel generators. The load growth in remote areas has raised some concerns. There are around 300 remote areas across Canada, with a total population of around 200,000 people. There are many concerns regarding the reliability of isolated microgrids as load increases, and energy management when introducing renewable energy sources such as wind and PV. In addition, the vital role played by the energy storage systems (ESS) which would improve the reliability of the system by mitigating the uncertainty of the output power of wind turbines and solar panels. Thus, ESSs bring a flexibility and robustness to the system though it will add more complexity to the energy management of the system. A study in [22] investigated placing renewable energy alternatives in remote communities in northern Ontario, Canada, which would result in reducing the dependency on diesel generators. As a result, mitigating fuel consumption, operating costs, and $CO_2$ gas emissions was achieved after a study of six scenarios was presented.

Indeed, the intermittent nature of renewable energy is inevitable so the forecasted data for wind speed and PV insolation lacks some accuracy. Therefore, there is a need to consider uncertainties in the operations models. Uncertainties of operation in power systems can be categorized into outages of generation units and departure from forecasted values [23]. A number of related research works have been reviewed in this thesis, as follows:

Energy management of various ESSs was considered in [24], such as batteries and water tanks, considering the randomness of solar insolation and load profiles, in order to reduce the average energy cost of a smart building and determine the best combination and optimal capacities of storage devices. This problem formulation was solved by a scenario tree method, where the scenarios generated by Monte Carlo simulation (MCS) are organized in a tree structure to mitigate the computational time needed.

In order to capture the randomness of a load over time, an adaptive energy consumption scheduling strategy with online stochastic iterations were proposed in [25]. This strategy was tested on a distribution system with connected microgrids. A multi-objective function that minimized the cost and peak to average demand ratio was considered.

Dukpa *et al.* [7] proposed a fuzzy optimization approach to optimally schedule the output energy of wind turbines while employing ESS for participating in the day-ahead unit commitment problem. The uncertain nature of forecasted wind speed was considered, and the approach utilized was a Weibull distribution. The authors concluded that ESS helps the system during high wind energy output and low price by storing the energy. Also, when there is a deficit in wind energy output, ESS delivers enough energy and acts in away similar to the classic spinning reserve.

In [26], a resource scheduling problem as a multi-scenario linear optimization problem was formulated. The idea of using EVs either as loads, sources, or storage devices was studied, and the V2G impact on minimizing the operating cost and emission was illustrated. Various uncertain parameters were considered, such as power demand, wind power, solar power, and PEV charging. A particle swarm optimization (PSO) approach, was applied to achieve successful scheduling for a tested system.

## 1.3 Research Objectives

This main objectives of the research presented in this thesis involves studying the impact of charging PEVs, DR options, and energy management in an isolated microgrid. The research objectives are outlined as follows:

- Develop a comprehensive mathematical optimization model for scheduling and operating isolated microgrids considering the modeling of PEVs, BESSs, and DR options in the presence of solar and wind energy resources.
- Examine the impact of coordinated *vis-à-vis* uncoordinated charging of PEVs, and the impact of DR options on an isolated microgrid operation, considering various operational cases and scenarios.
- Develop a stochastic optimization model for energy management considering the charging load of PEVs, and study the impact of uncertainty of different parameters. The uncertainty of demand, output generation of wind turbines and PV panels, and the initial SOC of a PEV battery at the start of charging will be examined after developing a comprehensive modeling framework.

## 1.4 Thesis Organization

The thesis is organized as follows:

The background of this work is identified in Chapter 2. A general overview of the smart grid and the various types of EV that are available in the market are provided. The charging levels that are used to power EVs are discussed as well. Furthermore, the importance of DSM and DR and their strategies have been explained in detail. Finally, Chapter 2 reviews some uncertainty handling approaches that are applied in power system operations.

Chapter 3 shows the mathematical model of the isolated microgrid operation. The mathematical model includes the formulation of OPF, BESSs, DR, PEVs, and related operating constraints. Various objectives are applied, and two PEVs charging strategies are adopted. Finally, the results and analysis of different cases and sceneries are discussed in detail.

Chapter 4 presents four different cases to handle a novel stochastic short-term operations model of the isolated microgrid considering variable/fixed DR and PEV charging loads. The stochastic nature of wind and solar generation output as well as the uncertain energy consumption patterns of customers is investigated; the uncertainty of the SOC of the PEV battery at the start of charging is included in the stochastic model.

The research work is summarized and conclusions are drawn in Chapter 5. Also, Chapter 5 points out some suggestions for future research on smart microgrids.

# Chapter 2

# Background

## 2.1 Introduction

Chapter 1 presented the motivations, research objectives, and a detailed review of literature pertaining to the topics related to this research work. Moving forward, this chapter provides a background review on the subject, the tools, and the models that correlate with the research objectives. Section 2.2 presents a background on smart grid and microgrids. It is followed in Section 2.3 by a comprehensive overview of different types of EVs, the charging levels that have been utilized, and the modeling and the schemes of PEV charging. Section 2.4 discusses various strategies of DSM. A brief description of the optimization methods that have been used in this research work is also included in this section. Finally, tools and approaches that deal with uncertainties are briefly discussed.

## 2.2 Smart Grid

The electric grid infrastructure has managed to serve mankind's needs successfully, unchanged for almost a century. Nevertheless, as the electric grid infrastructure is unavoidably ageing it becomes less efficient. As a result, the need to modernize the grid to be more sustainable, reliable, affordable, efficient, convertible, environmentally friendly and secure is becoming a clear and a challenge at the same time [27]. There are various differences between the existing electric power grids and smart ones. Table 2.1 presents a brief comparison between them [28]. For these reasons and more, extensive research has been carried out around the world to formulate a new vision for the future of smart power grid [29]. Smart grid is defined by the European

Table 2.1: Brief Comparison Between Traditional and the Smart Grid

| **Traditional Grid** | **Smart Grid** |
|---|---|
| Electromechanical | Digital & Electromechanical |
| One-way communication | Two-way communication |
| Centralized generation | Centralized & Distributed generation |
| Few sensors | Sensors throughout |
| Manual monitoring | Self-monitoring |
| Manual restoration | Self-healing |
| Failures and blackouts | Adaptive fault clearing and islanding |
| Limited control | Pervasive control |
| Few customer choices | Many customer choices |

Technology Platform of Smart Grid (ETP) as a new concept electricity network, from the point of generation until the point of consumption, that is intelligently capable of exchanging electricity and information among the components of the electric grid. Furthermore, it has the ability to monitor and react instantly to any change in the electric grid, beginning from the generation at power plants and ending with customers' preferences [30]. There is, however, no universally accepted and applicable definition of a smart grid. Nevertheless, a smart grid is expected to have the following features [31]:

1. Improved power reliability,

2. Accommodation of DG sources,
3. Use of a wide range of RES,
4. Improved resilience against disturbances,
5. Mitigation of the operating cost of utilities,
6. Lower GHG emissions,
7. Self-healing responses to disturbances and better self-management,
8. Introduction of consumer participation,
9. Integration of PHEVs and ESSs.

A smart grid will be equipped with AMI in order to enhance DSM and energy efficiency [31]. In [32], the potential benefits of utilizing smart metering technologies have been highlighted and a brief summary of the legal framework for controlling metering technology in Europe is provided. In the U.S.A, the National Institute of Standards and Technology (NIST) has set a framework to coordinate the research on smart grids. This coordination would achieve interoperability of smart grids [34].

### 2.2.1 Microgrid

The introduction of smart grids has led to the development of a new grid paradigm referred to as a microgrid. Basically, large scale of penetration of DG sources has stimulated the development of microgrids. A microgrid is considered to be the cornerstone of a smart grid system [30].

A microgrid is defined as a cluster of loads and micro-generation technologies, such as microturbines (MT), fuel cells (FC), diesel generators, PV panels, and wind turbines, together with energy storage devices, such as flywheels, energy capacitors, batteries, and controllable loads, *i.e.* EVs, operating as a single controllable entity that provides both power and heat to its local

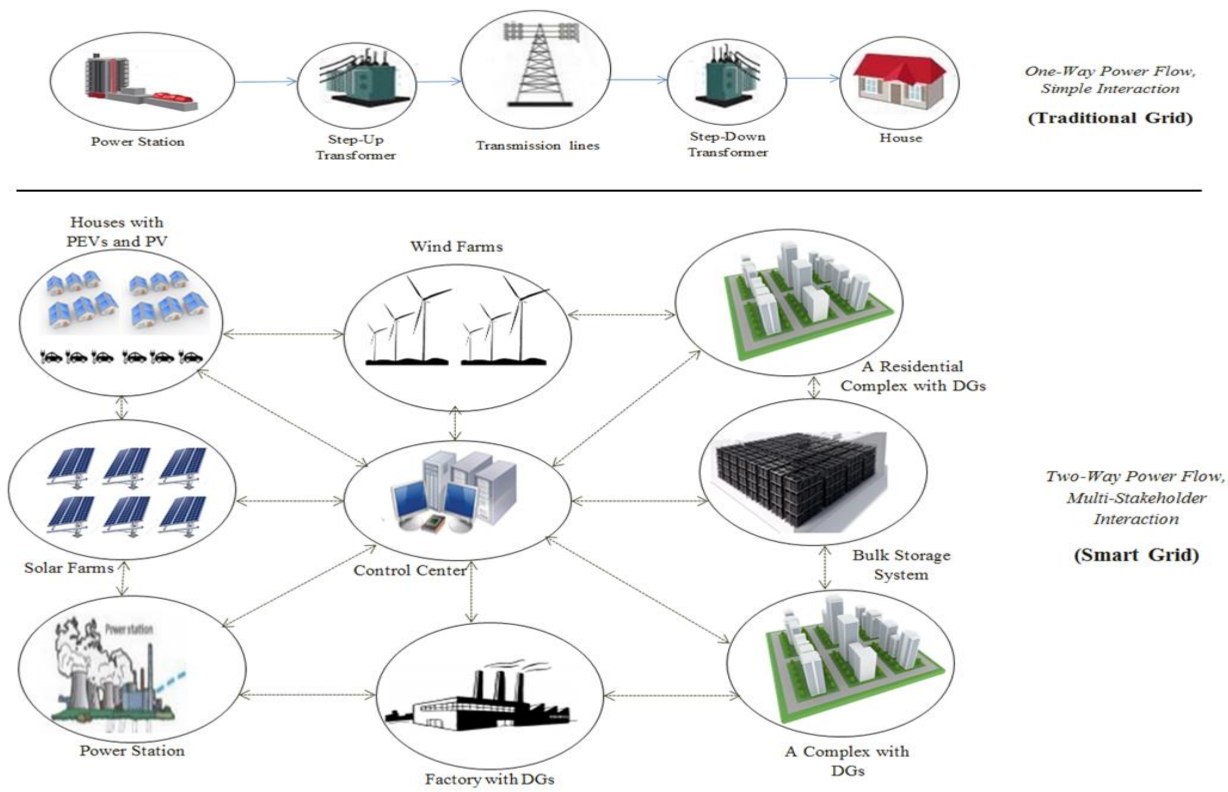


Figure 2.1: AN EXAMPLE OF THE TRADITIONAL POWER GRID VS SMART GRID [33]

area. Microgrids present a new paradigm of operation of DG units and have the ability to operate either in grid connected or isolated mode [35]. The key factor that differentiates a microgrid network from a distribution network is the implementation of control. The microgrid is either connected to the main grid through a point of common coupling (PCC) or isolated from the main grid either because it is in a remote area and the microgrid operates in isolation or in case of faults, disturbances, and natural disasters.

*Microgrid Projects*

There are many examples of ongoing microgrid projects around the world. A 100 kW capacity microgrid has been developed and is under research at the Consortium for Electric Reliability

Technology Solution (CERTS) test bed near Columbus, Ohio, U.S.A. Another example of an ongoing microgrid projects is Fort Sill in the U.S.A. This huge project has a rating of 0.480 kV, 60 Hz, and total capacity of 630 kW; in addition, it has an energy storage capacity up to 250 kWh, a 30 kW solar PV system, and a 2.5 kW wind turbine. In Bronsbergen Holiday Park, Netherlands, the first microgrid was built in order to improve the power quality of a residential area. Solar PV panels have been installed over the roof tops of 108 houses [36].

In Japan, the Aomori microgrid project in Hachinohe was developed to house 150 kW capacity of weather-dependent generation, such as PV and wind turbines, along with a 510 kW capacity of controllable digester gas engines, and ± 150 kWh capacity of lead-acid BESS [37].

The pilot project on single phase isolated microgrid in a Greek island of Kythnos is installed to house a capacity of 10 kWp of PV, 53 kWh of BESS, and a diesel generator that has a nominal output of 5 kVA. In addition, each house in the isolated island is supplied by 2 kWp of PV system and 32 kWh of battery storage bank [38].

**Battery Energy Storage Systems**

BESS is playing an important role in the microgrid operations. Basically, there are two paradigms of BESS operation, load-following and price-following. Technically, the output power of the load-following paradigm of BESS responds to any random change in the load profile, such as a changing balance between generation and demand. The price-following involves buying energy when the cost is low to charge the battery, and selling the energy later when the cost of energy is high. Indeed, BESS has the ability to offset the RES fluctuation due to the intermittent nature of wind and PV [35, 36]. BESS are usually used as a backup to balance the mismatch between generation and loads; however BESS can do more than that. For instance, it has the capability to mitigate the effect of intermittency of PV and wind power. When there is a surplus energy from PV or wind, it will be stored in the BESS and used later, whereas there is a shortage of energy caused by either PV or wind to supply the demand, the stored energy in the BESS will be discharged to make up for the deficit [36].

Essentially, one the main advantages of BESS is its ability to transform the uncontrollability and unpredictability of the wind and PV sources into controllable and predictable ones [39].

### Renewable Energy Sources

There are various types of RES that are considered to be environmentally friendly and provide free energy. These can be either in a large-scale on-grid projects or small-scale off-grid projects. Tidal, wave, solar, wind, hydro, geothermal, and biomass energy are examples of RES. In this thesis, only two types of RES are considered, wind and solar energy, both typically located in small-scale off-grid projects. In Canada, there are about 300 remote communities that house 200,000 people, and their main source of energy comes from fossil fuel generators. Recently, wind and solar energy penetration has been increasing in order to reduce the dependency on fossil fuel, reduce cost, mitigate gas emissions, and harness free and clean energy [22].

*Wind Energy*

According to the Canadian Wind Energy Association (CANWEA), the lead province in generating wind power up to December 2014 is Ontario. The installed capacity of wind turbines is more than 2,400 MW in Ontario, which supplies around 3% of the total provincial demand [40]. The installed wind turbines are used to harness the energy from wind. Based on the wind speed at a certain site, the output power that can be generated by wind turbines utilizing the wind turbines' characteristics are given by the following equations [41]:

$$P_W(v) = \begin{cases} 0 & 0 \le v \le v_c \\ S(v) & v_c \le v \le v_r \\ P_W^{Rated} & v_c \le v \le v_0 \\ 0 & v \ge v_0 \end{cases} \tag{2.1}$$

where the function $S(v)$ can be calculated below 2.2, and depends on the wind speed between the cut-in and cut-out limits:

$$S(v) = P_W^{Rated} \cdot \left[ \frac{v - v_c}{v_r - v_c} \right] \tag{2.2}$$

where $v_o$, $v_c$, and $v_r$ are the cut-out, cut-in, and rated wind speed of a wind turbine, respectively, and $v$ denotes a measured wind speed at an instant. $P_W(v)$ is the output power of a turbine corresponding to instantaneous wind speed, and $P_W^{Rated}(i)$ denotes the rated output power of a wind turbine, at bus $i$.

*Solar PV Energy*

The rapid development in solar PV energy technology in recent years has reduced the cost of manufacturing PV panels, and indicates that solar energy will gain a considerable percentage share of electric power generation in the near future [42]. The output power that can be generated by PV panels depends on the solar radiation during a day. The equation below can be used to determine how much power a PV module can generate [43]:

$$P_{PV} = P_{PV}^{Rated} \cdot D_f \cdot \left( \frac{R_t}{R_{standard}} \right) \cdot \left[ 1 + \zeta_p \left( T_{PV} - T_{standard} \right) \right] \tag{2.3}$$

where $D_f$ represents the component de-rating factor, and $R_t$ and $R_{standard}$ denote the solar insolation during each hour and under a standard test condition, respectively. Moreover, $\zeta_p$ states the temperature certification of power, while $T_{PV}$ and $T_{standard}$ denote the PV panel temperature during each hour and under a standard test condition, respectively. Finally, $P_{PV}^{Rated}$ and $P_{PV}$ represent the rated capacity of each installed PV array and the actual output power extracted from PV arrays, respectively.

## 2.3 Electric Vehicles

The history of EVs goes back to 1834 when the first EV was invented. In the earlier 1900s, EVs outsold internal combustion engine (ICE) vehicles. After many years of success, however, their market share declined due to many reasons. The limitations of battery technology and the lack of power electronics technologies let ICE vehicles top the market. ICE vehicles offered superior advantages in terms of speed and driving range, whereas EVs suffered limitations in both characteristic. EVs almost vanished due to the dominance of gasoline engines since 1930. Nevertheless, when in the early 1970s, there was an energy crisis around the globe due to political reasons and many countries launched programs to develop EV technologies [44]. Nowadays, EVs have begun to be driven on the roads, thanks to developments in battery and power electronics technologies. These developments make it possible to close the range and the speed between ICE vehicles and EVs.

As the world moves forward to reduce environmental emissions, which is a prime factor in the global warming issue, public interest in using vehicles that have low or zero emissions has grown substantially [44].

### 2.3.1 Types of Electric Vehicles

*Plug-in Electric Vehicles*

A PEV is a type of EV that has no ICE on board, and is called a pure battery EV. These vehicles have battery packs that propel the electric motors. PEVs are charged by plugging the vehicles into an electric outlet power source; charging takes from half an hour to eight hours depending upon the level of charging. Even though PEVs do not emit tailpipe pollutants, the power plants where the power is produced may emit carbon dioxide or other gas emissions. Based on the USA Environmental Protection Agency (EPA) standard, PEVs are considered to be zero-emission cars as their motors do not produce any exhaust. The need for heavy and bulk batteries is one of the challenges that face PEVs. Also, the driving range of PEVs is only around 80 miles before they need recharging, while an ICE can go over 300 miles before refiling. Thus, there is a need for charging stations to charge the PEVs along the roads and highways [45, 46]. Many examples of PEVs exists, for instance, the Ford Focus, Nissan Leaf, and Tesla Model S.

*Hybrid Electric Vehicles*

An HEV is a type of EV that combines the benefits of both gasoline engines and electric motors. The batteries on board do not need to be plugged into an outlet charger; instead, they charge from the ICE during driving and regenerative breaking. The latter is a way of capturing the lost energy during braking and coasting by utilizing the motor as a generator. The energy is then stored in the batteries. This stored energy can be used later to supply extra power during acceleration. Furthermore, this extra power provided by the motor brings more benefits, such improving fuel economy without sacrificing performance, and reducing emissions. The Toyota Prius is the most-driven HEV [46].

*Plug-in Hybrid Electric Vehicles*

The PHEV is similar to an HEV, but with larger battery capacity and it has on board both an ICE and a battery. First, the PHEV is powered by the battery, but when the battery reaches its limits, the ICE starts operating to replace the electric drive train. The battery used in PHEVs can be charged in different ways: by plugging it into an outlet electric source at homes or stations, by the ICE, or through regenerative braking. Fuel cost saving in the PHEV depends on the driving mileages done by utilizing the battery only. It should be noted that if a PHEV never charges its battery from the grid, the fuel cost will be the same as for an HEV.

PHEV emissions are expected to be less than HEV ones since the former relies on a battery for some of the time. PHEVs can be driven for longer range than HEVs, which makes them suitable for long distance trips. Different companies manufacture different models of PHEVs available in the market in Canada, for example, the Ford C-MAX Energi, Ford Fusion Energi, and Toyota Prius Plug-in [45, 46].

### 2.3.2 Electric Vehicle Charging Levels

Charging of EVs requires an electrical outlet from which cars can draw power. The charging time needed to charge the batteries of EVs depends upon two factors: the depletion and the

SOC of the battery. The charging time can vary from 30 minutes to 20 hours depending on the type of the vehicle and the level of charging. Because charging EVs takes longer than fuelling conventional cars at gas a station, EV charging stations need to be most accessible where vehicles park for long hours, such as residential parking areas, workplace parking lots, shopping malls, and parking garages. Most modern charging equipment and vehicles are following a standard so drivers need not worry about the compatibility of their cars to connectors and plug receptacles. At the moment, there are three main charging levels, and one other is under development [44–46].

*Level 1*

Level 1 charging already exists in homes, which means no installation is needed. Level 1 uses the standard 110/120 V electrical wall outlet and provides power of up to 1.9 kW. Hence, Level 1 takes about 8−12 hours to charge an EV pack of batteries. EV owners usually plug in their vehicles to recharge the batteries overnight so that in the morning their vehicles are fully charged and ready to drive.

*Level 2*

Level 2 charging is utilized at both residential and commercial buildings. This type of charging is faster than Level 1, uses a 220/240 V electrical wall socket, and can charge power up to 19.2 kW. The time taken to recharge the battery of an EV is about 3-8 hours. All EV owners in Canada are expected to have either level 1 or level 2 charging capabilities. In this thesis, the charging level considered is level 2.

*Level 3*

Level 3 is also introduced an AC charging, but is different from Level 1 and 2 because it requires a 3-phase system. The nominal supply voltage of this level is between 208 − 600 V, with a maximum current of 400 A. This charging level is commonly used by commercial and industrial customers. It could be installed in homes too, but at a high cost.

*DC Fast Charging Level*

The DC fast charging level is mostly used at public charging stations, and has the ability to charge the battery of EVs in less than 30 minutes. The charger outlet power can go beyond 100 kW, and is considered a successful step toward minimizing charging times. It should be noted that DC fast charging level and Level 3 are still under development. Table 2.2 and 2.3 summarizes the generally accepted outlet standards and the mileage for the charging levels discussed. All the AC charging levels and DC charging level are summarized in Table 2.2.

Table 2.2: EVs Charging Levels: Outlet Standards [46]

| | Type | Current Range ($A$) | Voltage ($V$) | Power ($kW$) |
|---|---|---|---|---|
| **Level 1** | AC | 12 -16, 1-phase | 110/120 | 1.4 to 1.9 |
| **Level 2** | AC | Up to 80, 1-phase | 220/240 | Up to 19.2 |
| **Level 3** | AC | Up to 400, 3-phase | 208/600 | |
| **DC Fast Charging** | DC | Up to 200 | Up to 600 | 50 to 150 |

Table 2.3: EVs Charging Levels: Mileage [46]

| | Mileage / Charging Time | Primary Use |
|---|---|---|
| **Level 1** | 2-5 miles / hour of charging | Residential Charging |
| **Level 2** | 10-20 miles / hour of charging | Residential and Public Charging |
| **Level 3** | 60-80 miles / less than 30 minutes | Public Charging |
| **DC Fast Charging** | 60-80 miles / less than 30 minutes | Public Charging |

### 2.3.3 Modeling of PEV Charging Load Profile

In order to build a PEV charging load profile, it is essential to have enough data on how far and how long the cars are driven, and how long and where they are parked all day. Based on the 2001 National Household Travel Survey, vehicles are parked either at workplaces or at homes for more than 90% of the time [47]. A study carried out in [20] shows that PEV owners return home and start charging their PEV batteries at different times according to a normal distribution function with a mean at hour 18.00 and the variance of 1 hour. The authors in [20] utilized a Monte Carlo approach to simulate the daily driving distances for each EV, based on data taken from [47]. Therefore, the status of the SOC of PEV battery is determined by studying the PEV driving patterns. The beginning time of charging PEVs can be assumed to be consistent with the distribution of the vehicle's last trip ending.

### 2.3.4 PEV Charging Schemes

Charging of PEVs with high penetration would have a significant impact on a distribution system. Large unbalance charging would also have a negative effect on the infrastructure such as transformers. Moreover, it would have a detrimental impact if the charging with large penetration occurs in isolated microgrids which lack enough generation. Typically, there are two main ways to charge PEVs: uncoordinated and coordinated (smart) charging.

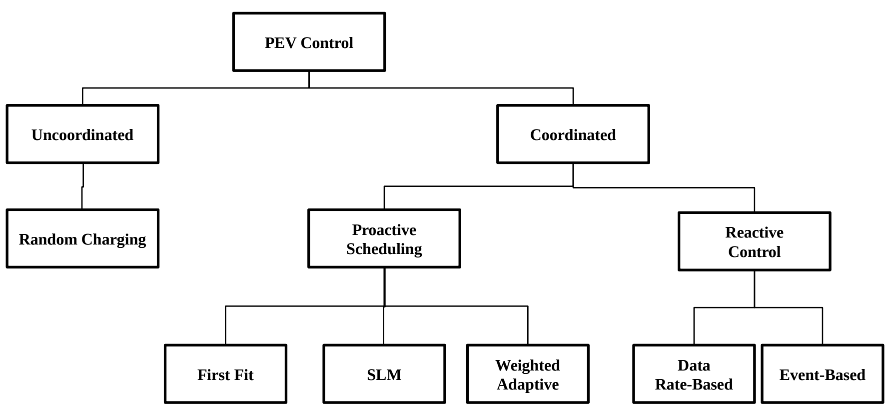


Figure 2.2: Coordinated and Uncoordinated PEV Solutions [48]

### Uncoordinated Charging

In this strategy, the charging pattern of PEVs is assumed to be random, and the PEVs owners do not have a smart metering technology. Normally, PEV owners immediately start charging once they return home in the evening. As a result, the charging load of PEVs will coincide with the peak demand of the system, which leads to an increase in the demand at the peak hours. This spike in the demand would affect a system's stability and security [6].

### Coordinated (Smart) Charging

Coordinated or smart charging assumes that PEV owners have a two-way communication infrastructure to receive control signals from the MGO. The charging hours of PEVs would be moved to off-peak hours or shifted to periods when the system is no longer under the threat of security or stability problems. Smart charging can be done by assuming that PEV owners are willing to participate in an energy management system, in return for economic incentives.

As seen in Figure 2.2, there are two main strategies to control coordinated charging: proactive scheduling and reactive control. Proactive scheduling searches for the first available time slot, first fit, to charge PEVs without violating the peak demand constraints whereas smart load management (SLM) determines the time slots in which to schedule the charging of PEVs based on maximizing the system operational performance [49]. The weighted adaptive scheduling strategy considers more parameters in an algorithm, such as price, charging delay, *etc*. The other scheduling strategy of charging PEVs is a reactive control protocol, which mainly reacts to a remarkable unforeseen deviation from the forecasted load profile. This significant deviation leads to grid problems, which must be avoided [48]. The reactive control technique works perfectly if there is a real time data interchange between the control panel and sensors; otherwise, the data will be outdated. Two approaches are proposed to overcome this synchronization issue: data-rate-based and event-based. The data-rate-based approach introduces a sensitivity parameter while sensors regularly send information to the control panel. When the sensitivity parameter increases, the probability of sending the information is outdated at the control panel. The latter sends the information to the control panel only when there is a change in the sensor measurement [48].

## 2.4 Demand Side Management and Demand Response

The interconnectivity and flexibility of different programs that facilitate customers to shift their demand during peak hours, and hence modify their energy consumption patterns and their load shape, is called DSM. DSM can be categorized into two main activities, DR programs, and energy efficiency and conservation programs [50]. DSM programs have been primarily utilities driven in the past, but are moving forward to be customer driven in recent years. DSM is envisaged to be a key component of the smart grid.

There are six load shaping techniques commonly refered to in the context of DSM: peak clipping, valley filling, load shifting, strategic conservation, strategic load growth, and flexible load shape, as shown in Figure 2.3 [51]. Peak clipping and valley filling techniques deal with mitigating the difference between the peak and the valley load level. These two techniques involve direct load control in order to flatten the load profile. The valley filling technique encourages end users to consume more energy at times when the price of electricity is low. Load shifting, which is widely utilized in distribution networks, is a technique used to shift the load from peak to off-peak periods, taking into consideration that the load is not dependant on time. For an overview of the recently applied DSM approaches in Asia, Europe, the U.S.A, and South America, the work in [52] could be of interest.

DR refers to a change in the usage of electricity by end-use customers from their normal consumption pattern, either in response to incentives or to the electricity price [53]. The interaction between the utilities and customers, involving interchanges of both energy and information, is realized in a smart grid through AMIs, which have two-way communication channels. As a result, the existence of both smart grid infrastructure and DR programs will mutually strengthen and help each other [54].

There are two simplest forms of DR. In the first, customers lower their demand during critical peak hours, but their demand during off-peak and mid-peak hours stays unchanged. Although

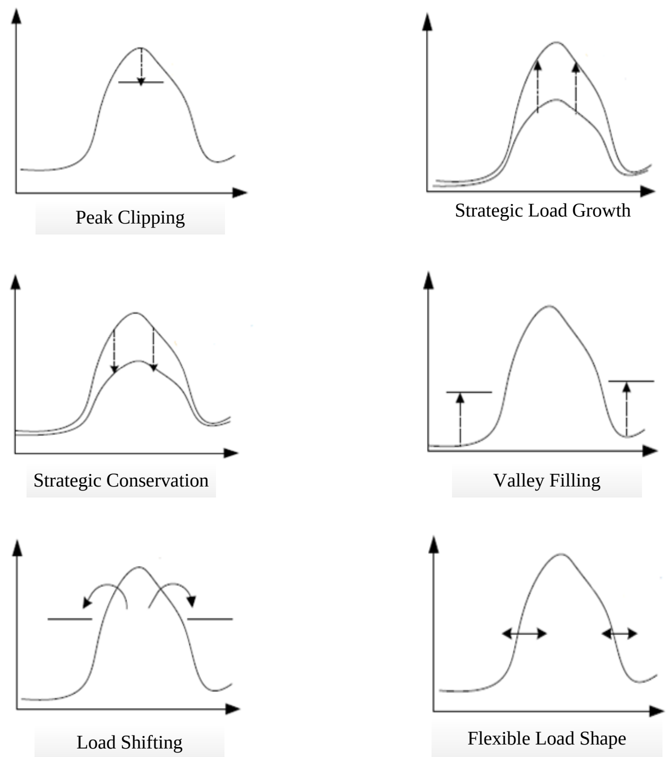

Figure 2.3: DEMAND SIDE MANAGEMENT TECHNIQUES

this could cause discomfort to customers, the microgrid operation cost will be decreased. In the second, customers shift some of their household demand from peak to off-peak hours in response to high electricity prices. They will bear no loss and incur no cost since the energy consumption is shifted from one time to another.

DR programs can be categorized into following programs [55]:

1. Incentive Based Programs
   (a) Classical
      i. Direct Load Control
      ii. Interruptible / Curtailable Load Management
   (b) Market Based

i. Ancillary Services Market
ii. Emergency Demand Response Programs
iii. Capacity Market Programs
iv. Demand Bidding Programs

2. Price Based Programs
   (a) Time of Use (TOU) Pricing
   (b) Critical Peak Pricing
   (c) Real Time Pricing

DR programs can profit both customers and utilities, and bring many advantages to the utility, in its distribution, transmission, generation, or in a microgrid system. DR plays a vital role by increasing the degrees of system flexibility, and improves the reliability and stability of the network.

In this thesis, demand shifting and load shedding are the two DR options considered. The goal of demand shifting is to move demand from peak periods to off-peak periods in order to level the demand profile and lower the microgrid's operation cost. Demand shifting would be possible if there are enough electric devices such as washers, PEVs, dryers that have a delay option. As a result, the load might be automatically delayed to other hours [7]. The load shedding is modeled to be in effect only if the total demand each hour exceeds the generation limits, and the system is not able to supply the demand.

## 2.5 Optimal Power Flow

In general, the OPF problem is an NLP problem that determines an optimal operating point for an electric power system in terms of a stated objective function [56]. Optimizing a desired objective function is subject to a set of equality and inequality constraints. An example of equality constraints is the power flow equations representing the correlation between power injections and voltages. Voltage limits, active and reactive power generation limits, and the flow on transmission lines are also examples of inequality constraints.

Many OPF objective functions can be used. Besides the minimization of generation cost, which refers to the classical economic dispatch problem, the minimization of the system losses or voltage deviation are examples of different objectives [57].

A general OPF formulation can be represented as follows :

$$\min_{x,u} \quad f(x,u) \tag{2.4}$$

$$\text{subject to} \quad g(x,u) = 0 \tag{2.5}$$

$$h(x,u) \leq 0 \tag{2.6}$$

$$x \in X, \quad u \in U$$

The function $f(x,u)$ is minimized and represents the system's objective and can include, for example, total losses or generation cost; $g(x,u)$ and $h(x,u)$ represents the vector function of equality and inequality constraints, respectively [57].

## 2.6 Uncertainty in Power System Operations

Scheduling the energy in the isolated microgrid operations after including RESs is mostly studied as a deterministic operation. However, capturing the stochastic nature of RESs, and taking into account the worst case scenarios becomes a necessity. Typically, the deviation from a forecasted value is represented as an error, which defines the randomness in a system and has a certain probabilistic distribution. According to [58], a fitting method is used to find the error's parameters that follows a standard probability distribution function such as normal distribution.

To generate scenarios for a system, a multi-stage tree model is developed in [58], as shown in Figure (2.4). The error in probability distribution function can be categorized as either continuous or discrete. The first can generate an infinite number of scenarios, which will impose a computational burden on the system operator, whereas the latter has the capability of discretizing the error into a finite number of samples [26].

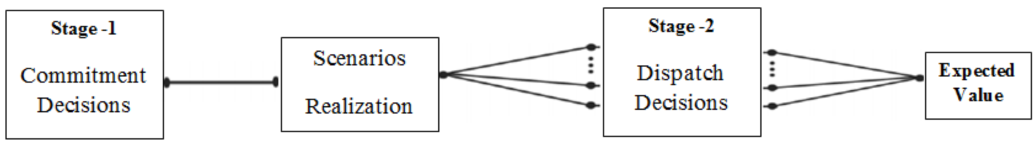


Figure 2.4: Two-Stage Decision Model

The MCS is usually used to generate large number of scenarios such as the demand and the output generation of wind and PV. A range of uncertainties associated with a likely probabilistic distribution profile of a given parameter are usually combined in order to find the expected value of the objective [26].

In case the probability distribution function forcasted error is discretized, the number of samples that are produced defines how many branches of each stage which at the end create the scenarios tree model. A general formulation of the optimization problem is described below to minimize the expected value of an objective function over a determined set of scenarios chosen in order to represent the range of uncertainty.

$$\min \quad E[\, f_0(x_i, u)\,]$$

$$\min \quad \sum_{i=1}^{S} \pi(x_i)\, f_0(x_i, u) \tag{2.7}$$

$$\sum_{i=1}^{S} \pi(x_i) = 1 \tag{2.8}$$

$$\text{subject to} \quad g(x_i, u) = 0 \tag{2.9}$$

$$h(x_i, u) \leq 0 \tag{2.10}$$

$$x \in X \tag{2.11}$$

where $f_0$ denotes the objective function, $g$ and $h$ are the constraint functions of an optimization problem, $x$ is the decision vector that should be within the set of $X$, and $u$ is the vector of specified stochastic variables [58]. Moreover, $\pi(x_i)$ represents the probability of each scenario that corresponds to a certain realization of $x$.

## 2.7 Summary

This chapter has summarized the background of smart grids and microgrids, and how they have altered the classic power system network. It has also discussed various types of EVs that have been on the market, and presented two main schemes for charging PEVs, and their impact on the microgrid network. DSM, which can boost the reduction of peak demand, and one of its programs, DR, which is used in this thesis, were discussed. The mathematical model of handling uncertainty, that is adopted in this thesis is provided, was briefly presented.

# Chapter 3

# Optimal Energy Management and Smart Charging PEVs in Isolated Microgrids

## 3.1 Introduction

As discussed in Chapters 1 and 2, the increased penetration of PEVs is a major challenge in the operation of microgrids due to the various negative impacts that are introduced, especially in isolated microgrids, when PEVs are charging. Thus, a proper scheme for charging PEVs would limit those impacts, and implementing DSM programs will further improve the performance of isolated microgrid operation.

This chapter presents a comprehensive mathematical model for short-term operation of an isolated microgrid. This model is used for optimal energy management combining generation from different resources such as diesel generators, wind turbines, solar panels, and BESSs and utilizing smart strategy to coordinate the charging of PEVs. The proposed model utilizes DR programs as well. Results of several cases and scenarios using the proposed model are analysed, to obtain insights into the effect of different charging techniques accompanied by DR programs.

## 3.2 Mathematical Model

This section presents the mathematical model for an isolated microgrid system operation.

### 3.2.1 Objective Functions

Various objective functions are combined to study the impact of adding PEV charging loads to an isolated microgrid, as follows:

*Minimize Total Loss:*

The benefits from minimizing the power losses of the system are fuel costs savings, reduced emissions, prevention of line overloads on system equipment, and decreased overall generation cost.

$$J_1 = \frac{1}{2}\sum_{t=1}^{T}\sum_{i=1}^{N}\sum_{j=1}^{N} G_{ij}\left[V_{i,t}^2 + V_{j,t}^2 - 2V_{i,t}V_{j,t}\cos(\delta_{j,t} - \delta_{i,t})\right] \tag{3.1}$$

In (3.1), $t$ is the index for time, $N$ denotes the total number of buses in the system, and $G_{ij}$ represents the conductance of the feeder $i - j$.

*Minimize Total Cost of Operation:*

This objective seeks to minimize the total operating cost of an isolated microgrid.

$$J_2 = \sum_{i=1}^{N}\sum_{t=1}^{T}\left(a_i Pg_{i,t}^2 + b_i Pg_{i,t} + c_i\right) + \sum_{i=1}^{N}\sum_{t=1}^{T} dVar_{i,t}^{up}\, Co_t^{DR} + \sum_{i=1}^{N}\sum_{t=1}^{T} P_{i,t}^{unmet}\, Co_t^{unmet} \tag{3.2}$$

The first term of (3.2) represents the operating cost of diesel generators, and the second term indicates the cost of shifting the demand through a payment made to the customers. The coefficient $Co_t^{DR}$ denotes the incentive paid by the MGO to customers for shifting their demand. The cost of unmet demand, if the demand cannot be served by the available resources at a certain hour, is represented by the third term. The coefficient $Co_t^{unmet}$ represents the cost of unmet demand.

*Minimize PEVs Charging Cost:*

From the PEV customers' point of view, minimization of the cost associated with PEV charging is the main objective. This objective can be used by the MGO to study the system impact of PEV charging, expecting rational behavior of customers, *i.e.*, customers seeking to minimize their charging costs. In this thesis, it is assumed that PEV customers are equipped with AMIs, and are subjected to real time pricing or TOU tariffs.

$$J_3 = \sum_{t=t_0}^{M} P_{ev,t}^{PEV}\, Co_t^{ch} \tag{3.3}$$

In (3.3), *ev* denotes the buses where PEVs are located, *M* represents the end hour of the charging period, when the vehicle batteries reach its full capacity, and $Co_t^{ch}$ is the price of charging the PEVs.

### 3.2.2 Isolated Microgrid Operational Constraints

The isolated microgrid system has a variety of small, modular electricity generation resources and each has its own set of constraints.

#### Generator Constraints

The active and reactive power generation from DG units is constrained by the units' upper and lower limits.

$$Pg_{min} \leq Pg_{i,t} \leq Pg_{max} \qquad \forall\, i \in N, t \in T \tag{3.4}$$

$$Qg_{min} \leq Qg_{i,t} \leq Qg_{max} \qquad \forall\, i \in N, t \in T \tag{3.5}$$

The power output from non-dispatchable sources such as wind and solar are fixed at their forecasted values, assuming that the forecast is perfect.

### Battery Energy Storage System Constraints

The BESSs need to consider the maximum power that can be drawn or injected during the charging and discharging processes [59, 60], as follows:

$$P_{i,t}^{BESS,ch} \leq P_{max}^{BESS} \, X_{i,t}^{ch} \qquad \forall\, i \in N, t \in T \tag{3.6}$$

$$P_{i,t}^{BESS,dis} \leq P_{max}^{BESS} \, X_{i,t}^{dis} \qquad \forall\, i \in N, t \in T \tag{3.7}$$

In each charge and discharge state, a certain amount of energy is lost because of the battery's internal resistance and energy conversion loss. This lost energy is accounted for by using the charging and discharging efficiency, as shown below, in the relations pertaining to the BESS energy stored at time $t$, $E_{i,t}^{BESS}$:

$$E_{i,t+1}^{BESS} = E_{i,t}^{BESS} + P_{i,t}^{BESS,ch} \, \eta^{in} \, \Delta h \qquad \forall\, i \in N, t \in T \tag{3.8}$$

$$E_{i,t+1}^{BESS} = E_{i,t}^{BESS} - \frac{P_{i,t}^{BESS,dis}}{\eta^{out}} \, \Delta h \qquad \forall\, i \in N, t \in T \tag{3.9}$$

Equation (3.8) represents the energy balance of a BESS while charging, taking into consideration the charging efficiency, $\eta^{in}$. Similarly, (3.9) describes the discharging period, taking into account the discharging efficiency, $\eta^{out}$; $\Delta h$ represents the time duration of each period. Furthermore, the BESS energy stored is constrained by the following conditions:

$$E_{min}^{BESS} \leq E_{i,t}^{BESS} \leq E_{max}^{BESS} \qquad \forall\, i \in N, t \in T \tag{3.10}$$

$$E_{i,t}^{BESS} \Big|_{t=0} = E_{S}^{BESS} \qquad \forall\, i \in N, t \in T \tag{3.11}$$

$$E_{i,t}^{BESS} \Big|_{t=T} = E_{F}^{BESS} \qquad \forall\, i \in N, t \in T \tag{3.12}$$

$E_{max}^{BESS}$ and $E_{min}^{BESS}$ in (3.10) represent, respectively, the maximum and minimum energy that can be stored in a BESS whereas $E_{S}^{BESS}$ and $E_{F}^{BESS}$ in (3.11) and (3.12) respectively are the initial and final energy status of the batteries.

Finally, the coordination between the charging and discharging to ensure decision variables is attained, that the batteries do not charge and discharge simultaneously, as per the following constraints:

$$X_{i,t}^{dis} + X_{i,t}^{ch} \leq 1 \qquad \forall\, i \in N, t \in T \tag{3.13}$$

**PEV Constraints**

The charging process of a PEV is limited by various constraints. The energy available in the battery of a PEV at an interval is given by the battery energy balance relation, as follows [14]:

$$E_{ev,t+1}^{PEV} = E_{ev,t}^{PEV} + \eta^{ch}\, P_{ev,t}^{PEV}\, \Delta h \qquad \forall\, ev \in N, t \in T \tag{3.14}$$

The PEV battery energy balance shown in (3.14) takes into account the efficiency of the charging process of the PEV, $\eta^{ch}$. The maximum power that can be drawn to charge the batteries of PEVs is limited by $\left(P_{max}^{PEV}\right)$, as given below:

$$P_{ev,t}^{PEV} \leq P_{max}^{PEV} \qquad \forall\, ev \in N, t \in T \tag{3.15}$$

$P_{max}^{PEV}$, in (3.15), is the maximum power that can be drawn from the electric outlets available at the customer's house, and depends on the level of charging installed.

As in the case of BESS, the energy stored in the PEV battery is subject to limiting constraints, as follows:

$$E_{min}^{PEV} \leq E_{ev,t}^{PEV} \leq E_{max}^{PEV} \qquad \forall\, ev \in N, t \in T \tag{3.16}$$

It is assumed that PEV battery energy level will not be allowed to fall below 20% of the total battery capacity [14].

The preferred PEV plug-out time constraint ensures that PEV batteries are fully charged before their preferred plug-out times when drivers leave for work, which in this thesis is assumed to be at 6 AM, as given below [14]:

$$E^{PEV}_{ev,t} = E^{PEV}_{max} \qquad \forall\ ev \in N,\ t = h_{po,t} \tag{3.17}$$

In order to estimate the load profile after PEVs are introduced into the system, the length of the PEV charging period needs to be calculated as follows:

$$Ct_i = N^{PEV}\left(E^{PEV}_{max}/P^{PEV}_{max}\right) \tag{3.18}$$

For example, from the above equation, if the capacity of a battery is equal 16 kWh, and knowing that plug-in outlet can charge up to 3.3 kW, the time needed for the PEV battery to become fully charged has to be at least 4.848 hours, assuming that $N^{PEV}$ is one.

**DR Constraints**

It is assumed that load shifting operation and its decision variables are determined and controlled by the MGO, not the end users. Also, the MGO has enough information on the appliances that are connected to its system, with an option of delaying them automatically; for instance, demand can be moved from one hour to another.

The variable $(dP_{i,t})$ is defined as the new demand at each hour after DR has taken place, and it can be equal to, more, or less than the base demand $(Pd_{i,t})$, as follows [7]:

$$dP_{i,t} \ = \ Pd_{i,t} \ + \ dVar^{up}_{i,t} \ - \ dVar^{dn}_{i,t} \tag{3.19}$$

$$\sum_{i=1}^{N}\sum_{t=1}^{T} dVar^{up}_{i,t} \ = \ \sum_{i=1}^{N}\sum_{t=1}^{T} dVar^{dn}_{i,t} \tag{3.20}$$

Balancing the demand variation during the day is defined by (3.20), which prevents the system from shifting customers activity to another day.

The maximum and minimum load that can be shifted from one hour to another, which are limited by the parameters $B_{up}$ and $B_{dn}$, which quantify the amount of shiftable load at each hour [7], are given by the following constraints:

$$0 \leq \; dVar_{i,t}^{up} \; \leq \; B_{up} \cdot Pd_{i,t} \tag{3.21}$$

$$0 \leq \; dVar_{i,t}^{dn} \; \leq \; B_{dn} \cdot Pd_{i,t} \tag{3.22}$$

### Demand-Supply Constraints

The power-flow equations for active and reactive power injection at a bus ensure a balance between the generation and demand at each hour and bus, as follows:

$$\begin{aligned} Pg_{i,t} + PW_{i,t} + PV_{i,t} + P_{i,t}^{BESS,dis} + P_{i,t}^{unmet} - P_{ev,t}^{PEV} - P_{i,t}^{BESS,ch} - dP_{i,t} \\ = V_{i,t} \sum_{j=1}^{N} V_{j,t} \left[ G_{ij} \cos(\theta_{ij,t}) + B_{ij} \sin(\theta_{ij,t}) \right] \end{aligned} \tag{3.23}$$

$$Qg_{i,t} - Qd_{i,t} = V_{i,t} \sum_{j=1}^{N} V_{j,t} \left[ G_{ij} \sin(\theta_{ij,t}) - B_{ij} \cos(\theta_{ij,t}) \right] \tag{3.24}$$

The active power balance shown in (3.23) accommodates the power generated by solar panels, wind turbines, discharging of BESSs, and diesel generators and the demand introduced by charging of BESSs, charging of PEVs, and the forecasted load at each bus and hour. The $P_{i,t}^{unmet}$ variable is introduced to reduce the imbalance between the generation and the demand, and adds a slackness to the system which helps the model arrives at a feasible solution.

The reactive power balance given by (3.24) shows that the reactive power requirements are met by diesel generators only.

#### Network Security Constraints

The voltage level at each bus and hour should be within the maximum and minimum specified limits, as follows,

$$V_{min} \leq V_{i,t} \leq V_{max} \tag{3.25}$$

#### System Peak Demand Constraint

To improve the isolated microgrid operation, the MGO imposes a PDC based on its total generation capacity such that the total peak demand at each hour does not exceed a specified limit.

$$Pd_{i,t} + dVar_{i,t}^{up} + P_{ev,t}^{PEV} + P_{i,t}^{BESS,ch} + J_{1,t} \leq PDC_t \tag{3.26}$$

It should be noted that $J_{1,t}$ denotes the losses at hour $t$.

## 3.3 Isolated Microgrid System Under Study

### 3.3.1 Microgrid System Topology

The analysis reported in this chapter is carried out considering the modified CIGRE microgrid benchmark system [61, 62], which is based upon an European medium-voltage distribution network benchmark. The 15-bus test system single-line diagram, at rated voltage of 10 kV, is shown in Figure 3.1, which is derived from the diagram presented in [61]. The network has a radial configuration, and there is no connection to the main grid thereby rendering the microgrid to be operating in isolated mode [61].

The DG unit at bus 1, functions as the main source of reliable power. The generation resources are confined to four types of distributed energy resources (DERs): diesel generators, wind turbines, solar PV panels, and BESSs. Details of the diesel generator, parameters, and their generation capacity are given in Table 3.1. The diesel generator operating cost parameters are obtained by assuming a diesel price of 1 $\$/lt$. The system has three diesel generators, with a combined capacity of 6,400 kW, solar PV panels with total capacity of 210 kW, and wind turbines of 1,400 kW (Table 3.2). The wind and solar PV output profiles for the isolated microgrid system are shown in Figure 3.2 [62]. There are three BESS units, each with a capacity of 900 kWh, and the efficiency of charging and discharging power being 90% [17]. Detailed information about the CIGRE system, such as its line parameters, *i.e.*, the resistance and reactance of the feeders, are provided in [60].

Table 3.1: DIESEL GENERATOR DATA

| Unit No. | Capacity | *a* | *b* | *c* |
|---|---|---|---|---|
| | kW | *lt* / kWh$^2$ | *lt* / kWh | *lt* |
| 1 | 2, 500 | 0.00001 | 0.224 | 45.5 |
| 2 | 2, 500 | 0.00001 | 0.224 | 45.5 |
| 3 | 1, 400 | 0 | 0.2571 | 25.5 |

### 3.3.2 Load Profiles

There are active and reactive power loads connected at each bus and these loads are either household or commercial. The 24-hour aggregated load profile at each hour is shown in Figure 3.3 [61], the peak demand occurs at hour 19, and the active power consumption at that hour is 7, 179 kW.

### 3.3.3 PEV Requirements

Bus 12 is a residential area, and there are 495 PEVs at this bus which draw charging power. Each PEV has a plug-in outlet capacity of 3.3 kW [46]. When PEV customers arrive home and are ready to charge their car batteries, the batteries have an SOC of 20%. The batteries cannot discharge their entire energy, because doing so, would lead to a reduction in their life span [46]. Table 3.3 presents the data of one type of PEV considered in this thesis [20, 63].

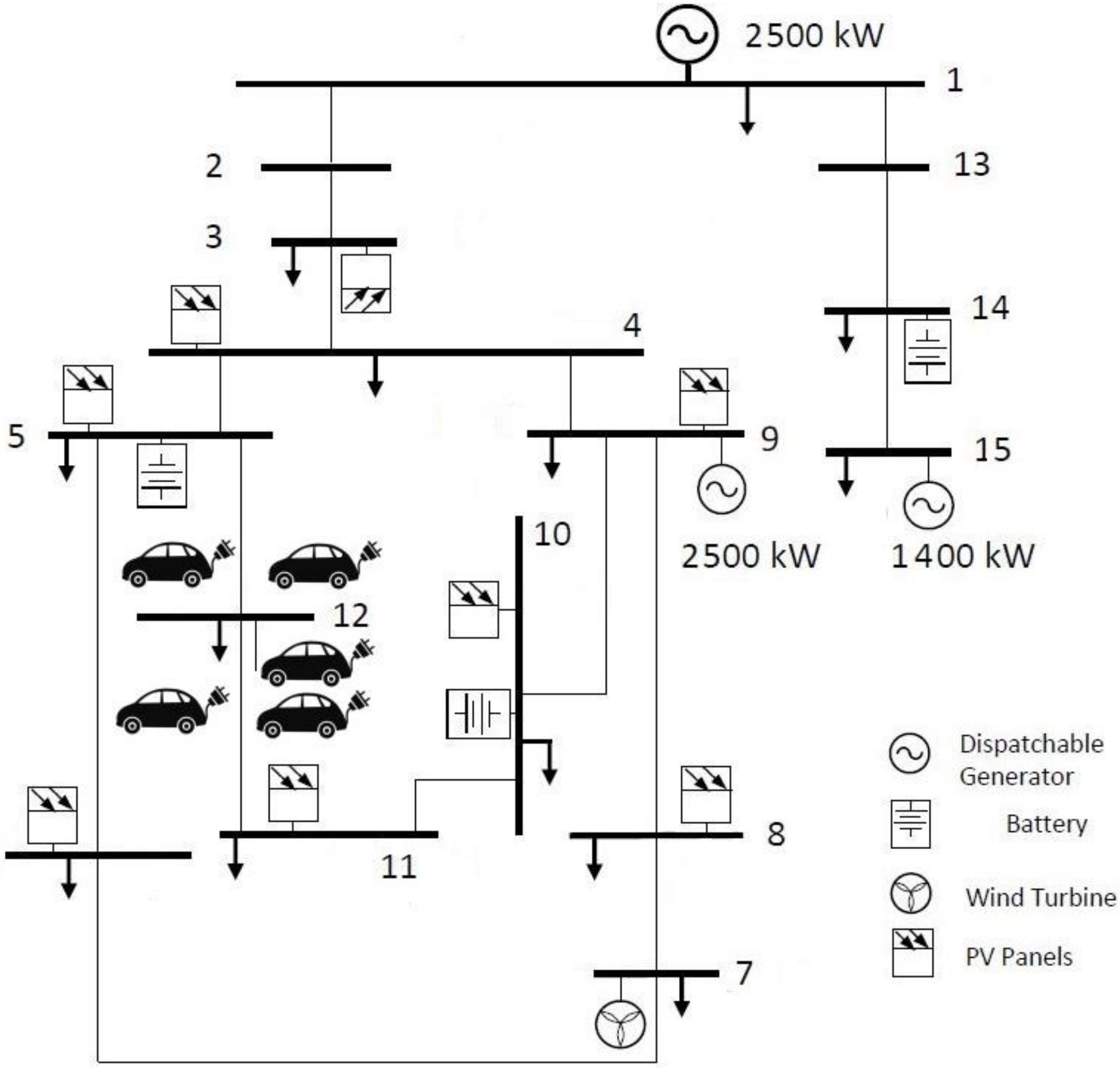


Figure 3.1: MICROGRID TEST BASED ON THE CIGRE-IEEE DER BENCHMARK MV NETWORK [62]

Table 3.2: Microgrid DER's Capacity

| Bus | DER Type | $P_{max}$ | Unit |
|---|---|---|---|
| 1 | Diesel Generator | 2,500 | kW |
| 3 | Photovoltaic | 20 | kW |
| 4 | Photovoltaic | 20 | kW |
| 5 | Photovoltaic | 30 | kW |
| 5 | Battery | 900 | kWh |
| 6 | Photovoltaic | 30 | kW |
| 8 | Photovoltaic | 30 | kW |
| 7 | Wind Turbine | 1,500 | kW |
| 9 | Diesel Generator | 2,500 | kW |
| 9 | Photovoltaic | 30 | kW |
| 10 | Photovoltaic | 40 | kW |
| 10 | Battery | 900 | kWh |
| 11 | Photovoltaic | 10 | kW |
| 14 | Battery | 900 | kWh |
| 15 | Diesel Generator | 1,400 | kW |

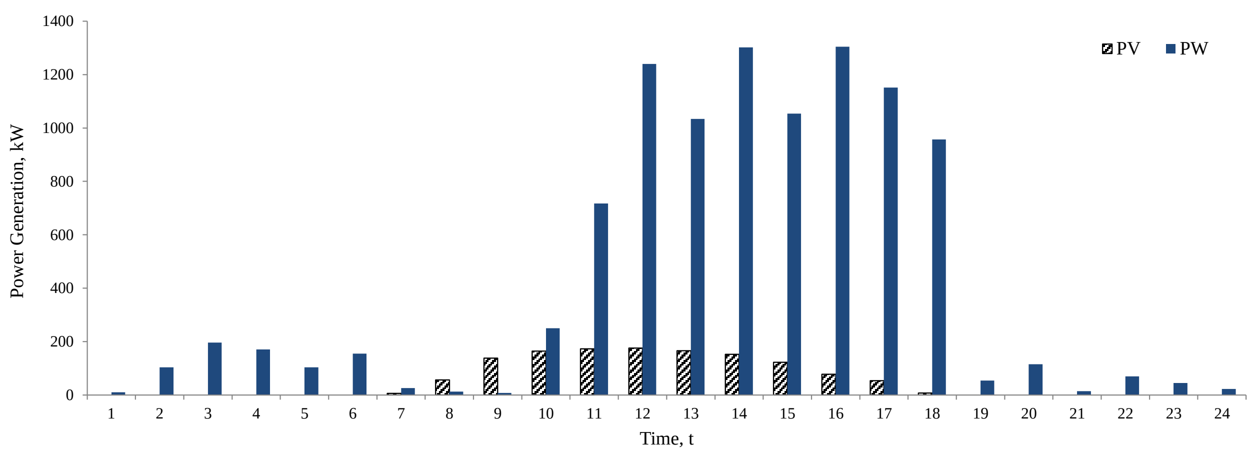


Figure 3.2: Wind and PV Output Power Generation Profiles

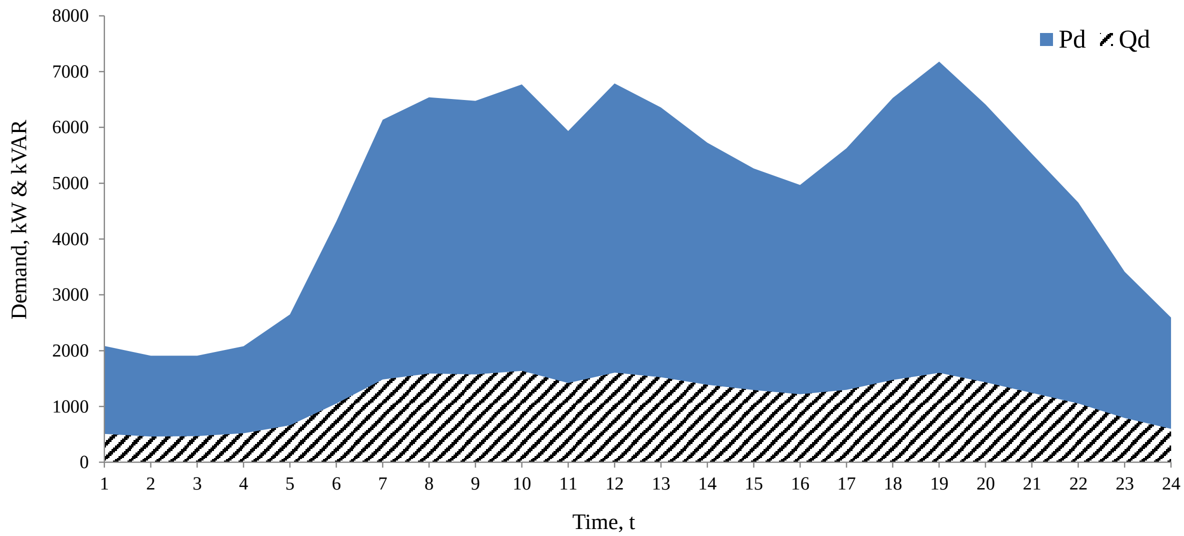


Figure 3.3: ACTIVE AND REACTIVE LOAD PROFILES

Table 3.3: GM CHEVY VOLT PEVS IN THE MARKET [63]

| Make & Model | Battery Size | Energy Available | All Electric Range | Charge Power |
|---|---|---|---|---|
| **GM Chevy Volt** | 16 $kWh$ | 3.2 $kWh$ | 40 $mi$ | 3.3 $kW$ |

When the battery of a PEV starts charging, there is some energy loss, and hence the energy needed is greater than the stated battery capacity. In this thesis, the PEV has a typical battery charger efficiency of 85% [20].

### 3.3.4 Time-of-Use Pricing

The price structure rate for the summer season in Ontario, Canada, is used in this work, as shown in Figure 3.4. As can be seen, the TOU prices coincide with the typical consumption profile of a customer in Ontario, and also depends on weather conditions. The TOU tariff has three different prices levels: on-peak, mid-peak, and off-peak. The peak hours are from 7 AM until 11 AM and from 5 PM until 7 PM; the mid-peak hours start at 11 AM and last until 5 PM in the evening;

while the off-peak hours are from 7 PM until 7 AM [64].

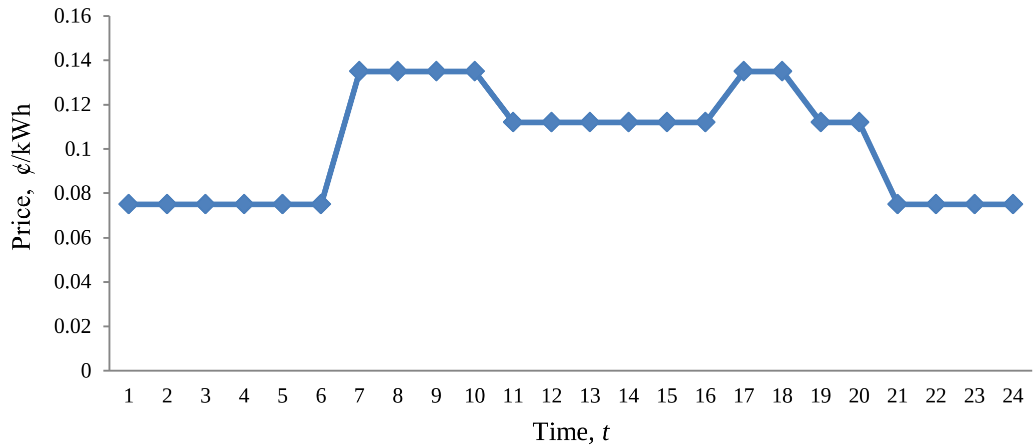


Figure 3.4: Ontario Electricity TOU Price Profile [64]

## 3.4 Definition of Scenarios and Cases

In order to investigate and evaluate the impact of smart charging of PEVs *vis-à-vis* uncontrolled charging in the presence of DR, three different cases and six scenarios have been simulated on the CIGRE isolated microgrid system.

### 3.4.1 Base Case

In this case, neither PEVs nor demand shifting are considered; the mathematical model developed in Section 3.2 is applied on the CIGRE microgrid system with an objective of minimizing the MGO cost.

### 3.4.2 Case 1: Impact of Uncontrolled and Smart Charging of PEVs

This case studies the impact of uncontrolled charging of PEVs in isolated microgrid operation and how smart charging of PEVs can help to reduce the adverse impacts of uncontrolled charging.

Two scenario (S1 and S2) are constructed to represents uncontrolled charging, where it is assumed that all customers start charging their vehicles simultaneously without considering the system operating constraints, and the MGO has no control on the charging of PEV. The PEVs are charged in the shortest possible time after plugging in, which is about four and half hours, considering the efficiency of the battery. It is assumed that the customers are aware of the different costs of charging at peak hours and off-peak hours, as per the TOU price [64].

***Scenario S1**: Uncontrolled Charging with No Objective Function or Operating Constraints*

This scenario effectively represents the worst case scenario since the PEV charging periods coincide with the system peak demand hours. All customers start charging their vehicles simultaneously, as soon as they arrive home, at 6 PM.

***Scenario S2**: Uncontrolled Charging with an Objective Function, No Operating Constraints*

This scenario has the objective of minimizing the charging cost of PEVs, $J_3$. It is assumed that customers are equipped with smart metering equipment and can therefore schedule their PEV charging so as to minimize their cost, while the MGO has no control on the charging schedules. Table 3.4 summarizes the scenarios of the first case.

In the smart charging scenarios (S3, S4, and S5), the MGO dispatches control signals to its PEV customers, to start charging, while ensuring that its operational constraints are not violated. The MGO imposes the PDC (3.26) so as to ensure that no new peaks are created when PEV charging loads are scheduled.

***Scenario S3****: Minimize Total Loss*

In this scenario, the MGO sets an objective to minimize the total power losses over 24-hours, as per (3.1), and determines the optimal schedules for the charging of PEVs.

***Scenario S4****: Minimize the Total Cost of Operation*

In this scenario, the MGO seeks to minimize its total cost of operation over 24-hours, as per (3.2), to determine the optimal schedule for the charging of PEVs.

***Scenario S5****: Minimize the PEVs Charging Cost*

In this scenario, the MGO determines the optimal charging schedule of PEVs assuming that customers would seek to minimize their charging cost over 24-hours, as given in (3.3). This scenario is a 'smart' version of scenario S2. A summary of the five scenarios is presented in Table 3.4.

Table 3.4: DESCRIPTION OF CASES AND SCENARIOS

| | **Case-1** | | | | | **Case-2** |
|---|---|---|---|---|---|---|
| | **Uncontrolled Charging** | | **Smart Charging** | | | **Smart Charging with DR** |
| | **S1** | **S2** | **S3** | **S4** | **S5** | **S6** |
| Objective Function | No | $J_3$ | $J_1$ | $J_2$ | $J_3$ | $J_3$ |
| PDC | No | No | Yes | Yes | Yes | No |
| Voltage Limit | No | No | Yes | Yes | Yes | Yes |
| Charging Window, $t$ | $18-22$ | $1-6$, $18-24$ | | | | $1-6$, $18-24$ |

### 3.4.3 Case 2: Impact of DR on Smart Charging of PEVs

***Scenario S6**: Minimize the PEVs Charging Cost with DR*

In this Case, the MGO studies the impact of DR on smart charging of PEVs assuming that customers would seek to minimize their charging cost over 24-hours, as given in (3.3). Therefore, this similar to scenario S5 of Case-1, except that the MGO has the DR as an option for peak load management instead of the PDC of (3.26).

According to [7], to quantify the potential demand shifting is a difficult task because there is not enough studies available. In this study, the maximum amount of shiftable microgrid demand is varied over a range to examine the impact of DR on microgrid operation, by varying $B_{up}$ and $B_{dn}$ in (3.21) and (3.22), respectively.

## 3.5 Results and Analysis

As discussed in the previous section, three cases studies are carried out to examine the operational aspects of the isolated microgrid considering PEVs and DR. These cases examine the impact of smart charging *vis-à-vis* uncontrolled charging of PEVs in isolated microgrids with and without DRs. When the DR option is considered, the MGO can modify the load profile to cope with the limitation of generation resources in the system. An incentive of 2 \$/kWh is introduced in the objective function (3.2) to encourage customers to defer their demand, without causing any inconvenience for them. The cost of unmet energy is assumed to be 3 \$/kWh , which is chosen to be significantly higher than the diesel generators' operating cost, base electricity market cost, as well as the DR cost.

### 3.5.1 Base Case

In the Base Case, the MGO optimally schedules the dispatch of various generation resources to ensure that the demand of the system is met while satisfying all the operating constraints of the the isolated microgrid. Figure 3.6 shows that the isolated microgrid base load profile with no PEV charging loads, the optimal diesel generation, BESS discharging, and RES schedule as a consequence of the cost minimization optimization. Observe that the MGO has to discharge energy from BESS at the peak demand hour (hour 19) when all the diesel generators operate at their upper limits and there is very little energy from RES.

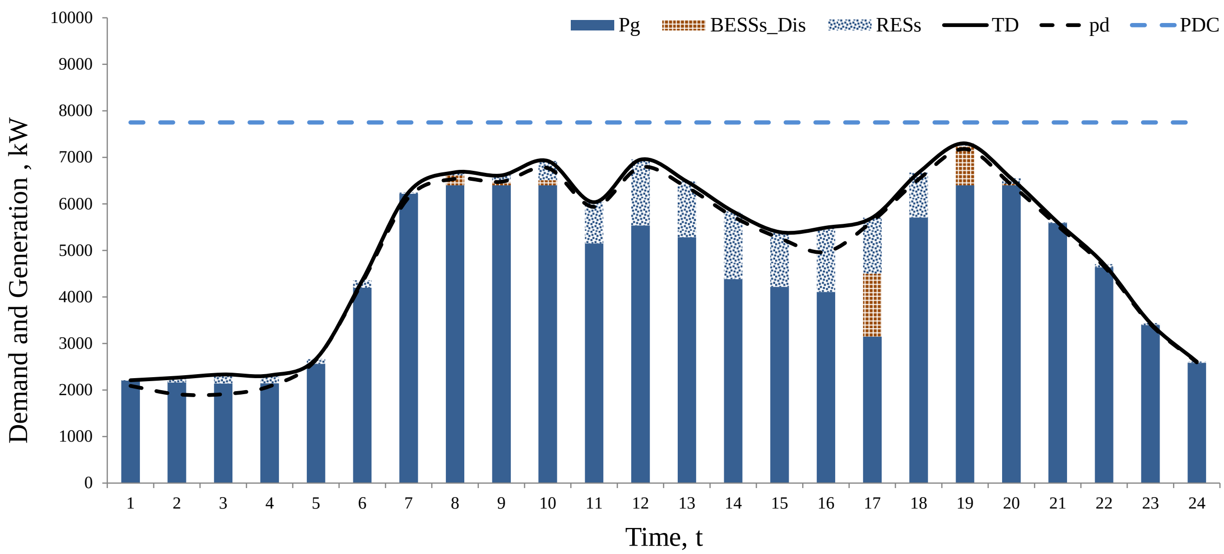


Figure 3.5: Total Generation and Demand Profiles for the Base Case

It should be noted that the PDC of (3.26) is not binding in this case since the peak demand of the isolated microgrid is always lower than specified limits.

### 3.5.2 Case 1: Impact of Uncoordinated and Smart Charging of PEVs

In the Base Case, the isolated microgrid has a peak demand of 7,179 kW at hour 19 as shown in Figure 3.3. In scenario S1, after introducing the PEV charging loads, the peak demand is increased significantly, by 1,634 kW at hour 19, and consequently there is unmet demand over four consecutive hours 18−21, as shown in Figure 3.7, implying that the MGO should shed some load or the transformers will be overloaded, leading to a failure in the system.

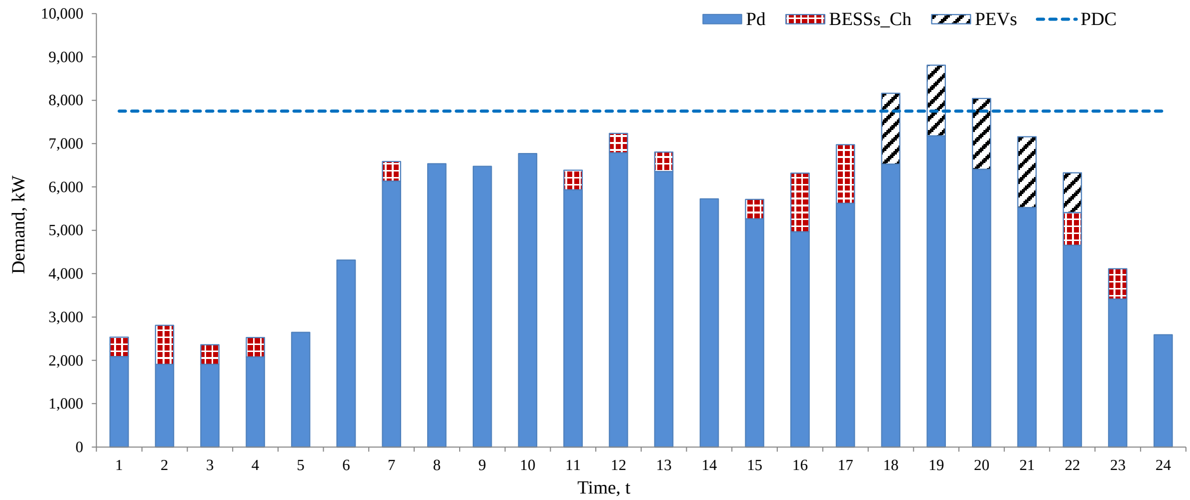


Figure 3.6: The 24-Hour Demand Profile for Scenario S1

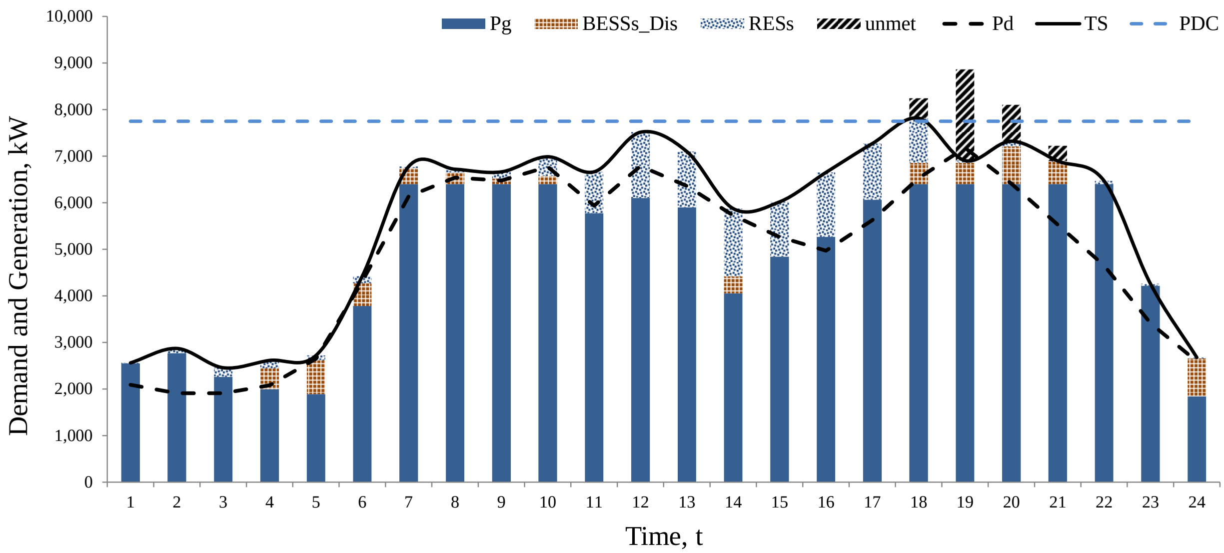


Figure 3.7: The 24-Hour Energy Schedule for Scenario S1

It is to be noted that BESS discharging is now required for several hours. Furthermore, to be noted that although the PDC of (3.26) is not included in Scenario S1, the microgrid demand exceeds the limit specified and results in unmet demand for few hours, as seen from Figure 3.6.

The isolated microgrid has an operating cost of 29,278 $/day when there is no PEV charging load, when PEVs are considered in Scenario S1, the total cost increases to 41,681 $/day, as shown in Table 3.5. This high increase in the total cost is mainly because of the large (3,492 kWh) unmet energy that is introduced by uncoordinated charging of PEVs which coincides with the peak demand hours.

Table 3.5: Summary Results of Uncontrolled PEVs Charging Scenarios

| | | | Uncontrolled Charging | |
|---|---|---|---|---|
| | | **Base Case** | **S1** | **S2** |
| **Total Cost for MGO** | $/day | 29,278 | 41,681 | 38,882 |
| **Diesel Generators Cost** | $/day | 29,278 | 31,861 | 31,601 |
| **PEVs Charging Cost** | $/day | 0 | 657 | 559 |
| **Unmet Energy Cost** | $/day | 0 | 10,477 | 7,840 |
| **Unmet Energy** | kWh | 0 | 3,492 | 2,613 |
| **Total Loss** | kWh | 1,962 | 3,756 | 3,458 |

Since Scenario S2 sets to minimize the charging cost of PEVs, customers are aware of the TOU prices. Accordingly, they shift the beginning of their charging period to hour 19 when the off-peak TOU price begins, as shown in Figure 3.8. The unmet energy is also shifted to hours 19, 20, and 21, and is decreased by 879 kWh because of the response of customers to the TOU price, as shown in Figure 3.9. The total PEV charging cost is reduced to 559 $/day compared to 657 $/day since the owners of PEVs try to minimize their charging cost by following the Ontario TOU prices. Therefore, the total cost of operating the microgrid in Scenario S2 is reduced to 38,882 $/day.

Both the uncontrolled charging scenarios demonstrate that uncoordinated charging is detrimental to the system, and the MGO needs to adopt smart charging to charge the PEVs in order to have a secure and reliable system.

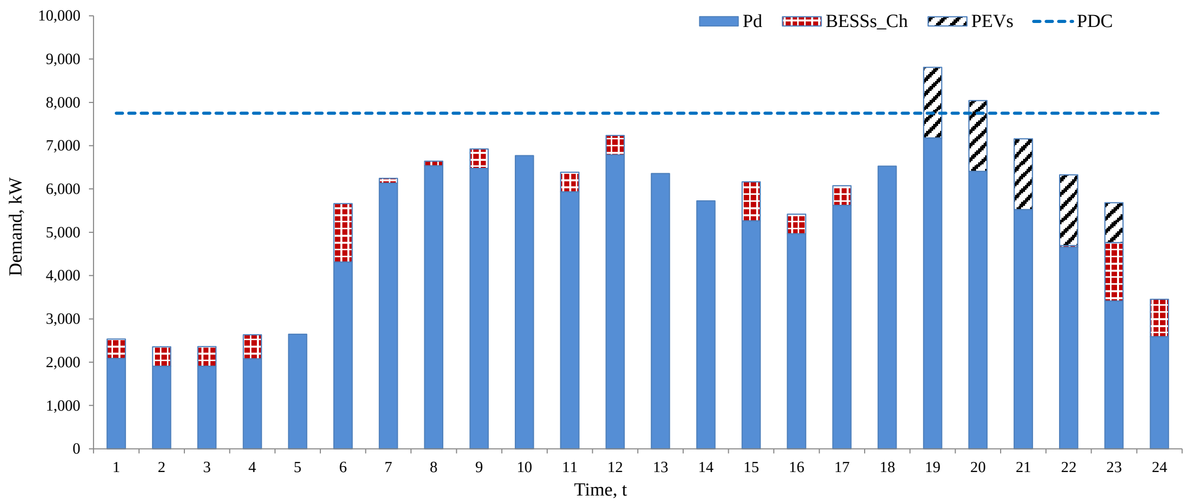


Figure 3.8: The 24-Hour Demand Profile for Scenario S2

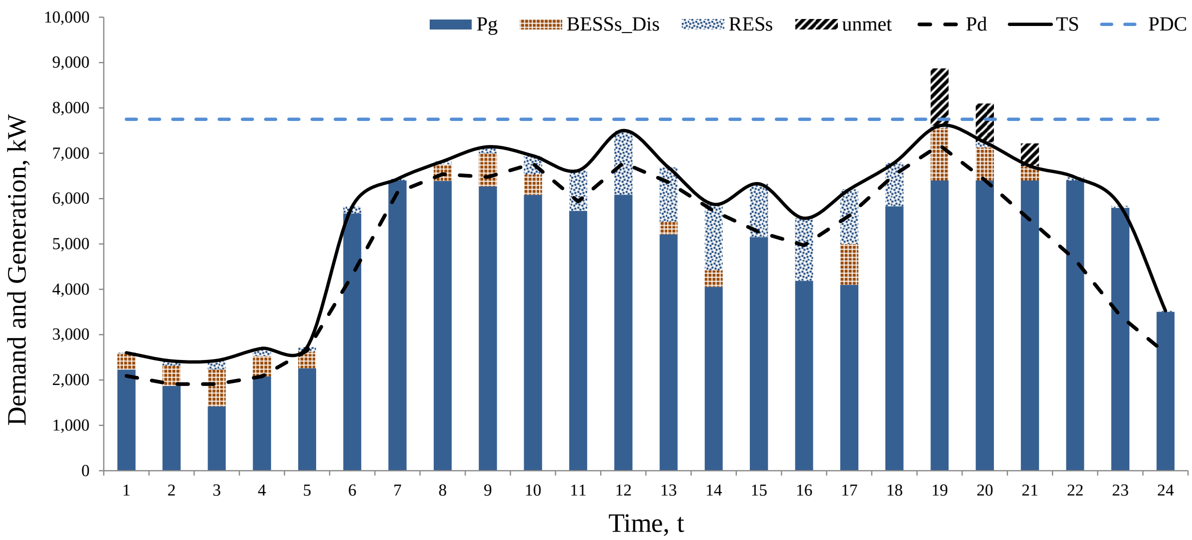


Figure 3.9: The 24-Hour Energy Schedule for Scenario S2

The different objective functions pertaining to the scenarios considered in smart charging represent both the MGO's (in S3 and S4) and the customers' (in S5) point of view. Smart charging benefits the system by shifting the charging periods and reducing the peak demand in a way that benefit both the MGO and customer.

After Scenarios S1 and S2 have been analyzed and evaluated, it is important to realize the need to impose the PDC (3.26) on this system, and hence find an optimal solution with no unmet energy while utilizing all the options available to the MGO, which in this case is the smart charging option.

The MGO in Scenario S3 optimally schedules the charging of PEV loads when the microgrid demand is low, in order to reduce the total losses of the system. The PEV charging load is now distributed across more hours compared to the Scenarios S1 and S2. It is noted from Figure 3.10 that the PEVs start charging during early morning hours, *i.e.*, from midnight to 5 AM, when the microgrid load is at its lowest level. From Table 3.6, it is noted that the utilization of smart charging reduces the power losses and hence the power quality of the system is improved. The loss is significantly reduced in Scenario S3 as compared to Scenarios S1 and S2, and is also lower than the Base Case, as per the MGO's objective.

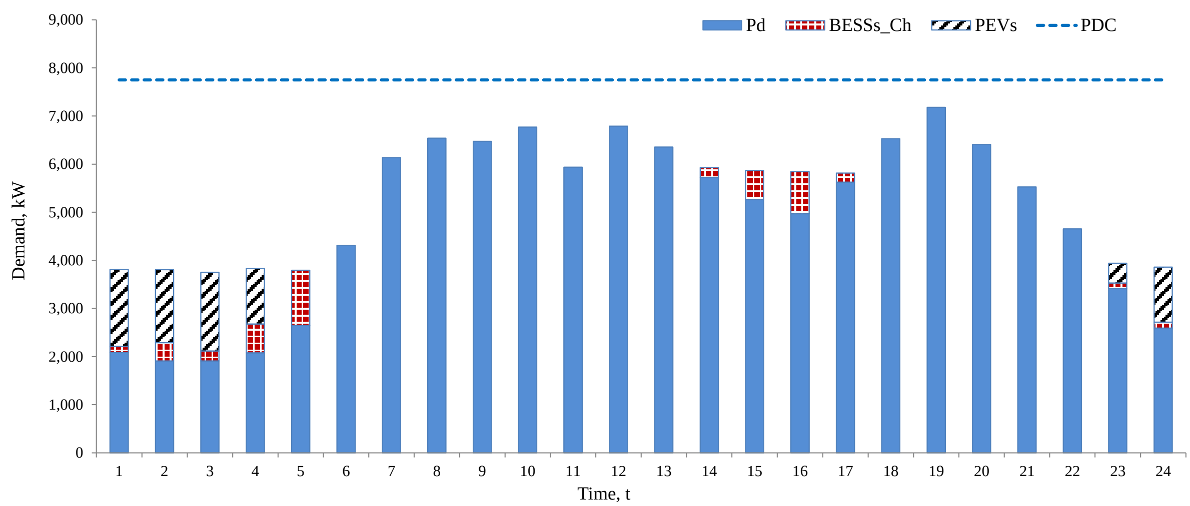


Figure 3.10: The 24-Hour Demand Profile for Scenario S3

There is no unmet energy in Scenario S3 since the start of PEV charging has been moved from 18 to 24 hours, as noted from Figure 3.11. This scenario results in a fairly flat load profile, without any new steep peaks at any hour, a result of PEV charging load periods being shifted from peak to off-peak hours in order to avoid any system overloading.

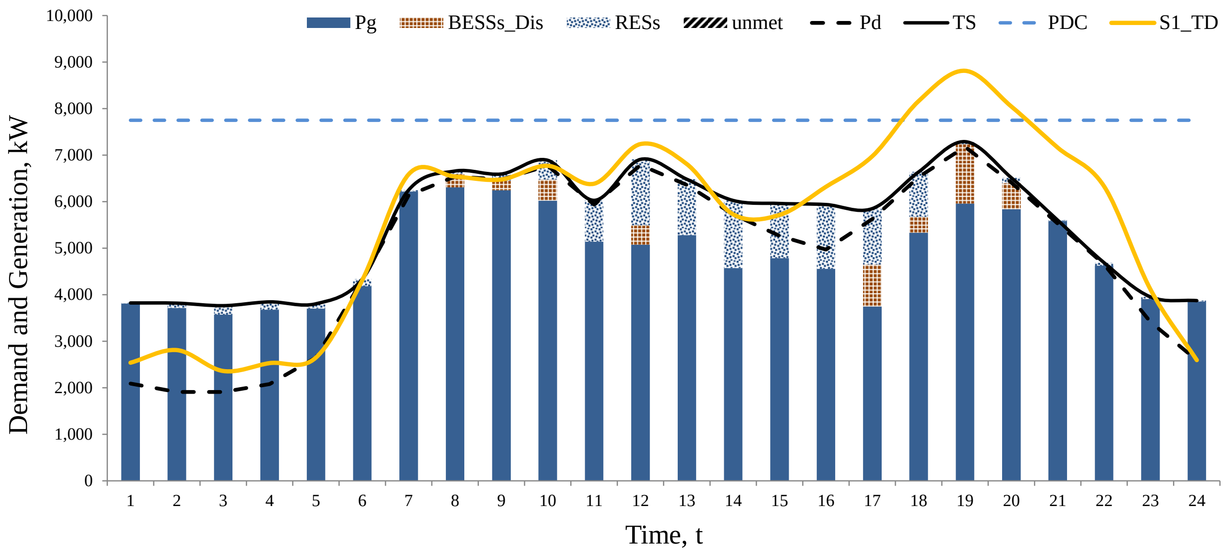


Figure 3.11: The 24-Hour Energy Schedule for Scenario S3

In Scenario S4, by coordinating the charging of PEVs, the MGO is able to manage the operation of the isolated microgrid such that its total operating cost is reduced while all operating constraints are satisfied.

In Scenario S4, the optimal scheduled charging periods of PEVs are similar to those in Scenario S3 because both the scenarios effectively seek to levelize the load profile (Figure 3.12). Nevertheless, the amount of load reduction in S4 is lower than that in any other scenario because of the cost minimization objective (3.2). It can be noted from Figure 3.13 that smart charging results in peak demand shaving by scheduling the charging of PEV loads to off-peak hours.

Table 3.6: SUMMARY RESULTS OF UNCONTROLLED AND SMART CHARGING SCENARIOS

| | | Uncontrolled Charging | | Smart Charging | | |
|---|---|---|---|---|---|---|
| | | **S1** | **S2** | **S3** | **S4** | **S5** |
| **Total Cost for MGO** | $/day | 41,681 | 38,882 | 30,970 | 30,632 | 31,834 |
| **Diesel Generators Cost** | $/day | 31,861 | 31,601 | 31,529 | 31,192 | 32,393 |
| **PEVs Charging Cost** | $/day | 657 | 559 | 559 | 559 | 559 |
| **Unmet Demand Cost** | $/day | 10,477 | 7,840 | 0 | 0 | 0 |
| **Unmet Energy** | kWh | 3,492 | 2,613 | 0 | 0 | 0 |
| **Total Loss** | kWh | 3,756 | 3,458 | 1,655 | 2,077 | 3,681 |

Moreover, as shown in Table 3.6, the total loss is relatively close to the Base Case, although it is greater than Scenario S3 as expected, since the objective is to minimize the total operating cost, not the loss. Figure 3.12 shows that the total microgrid demand is less than the PDC when the MGO considers smart charging whereas the total demand violates the PDC when uncoordinated charging of PEVs is used. The total operating cost for MGO is reduced in this Scenario S4 compared to others scenarios and it yields the optimal choice for both PEVs customers and the MGO.

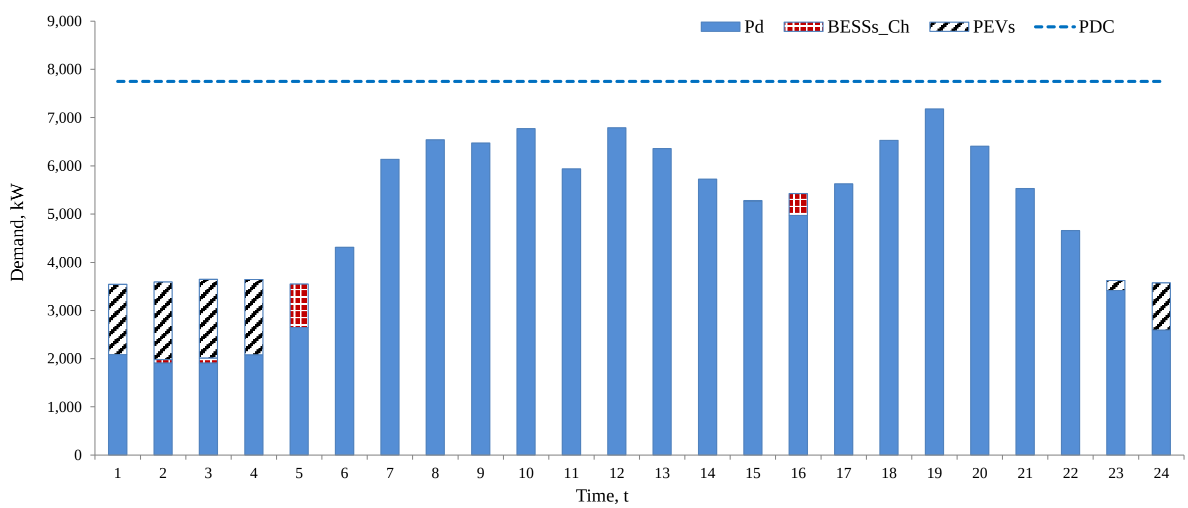


Figure 3.12: THE 24-HOUR DEMAND PROFILE FOR SCENARIO S4

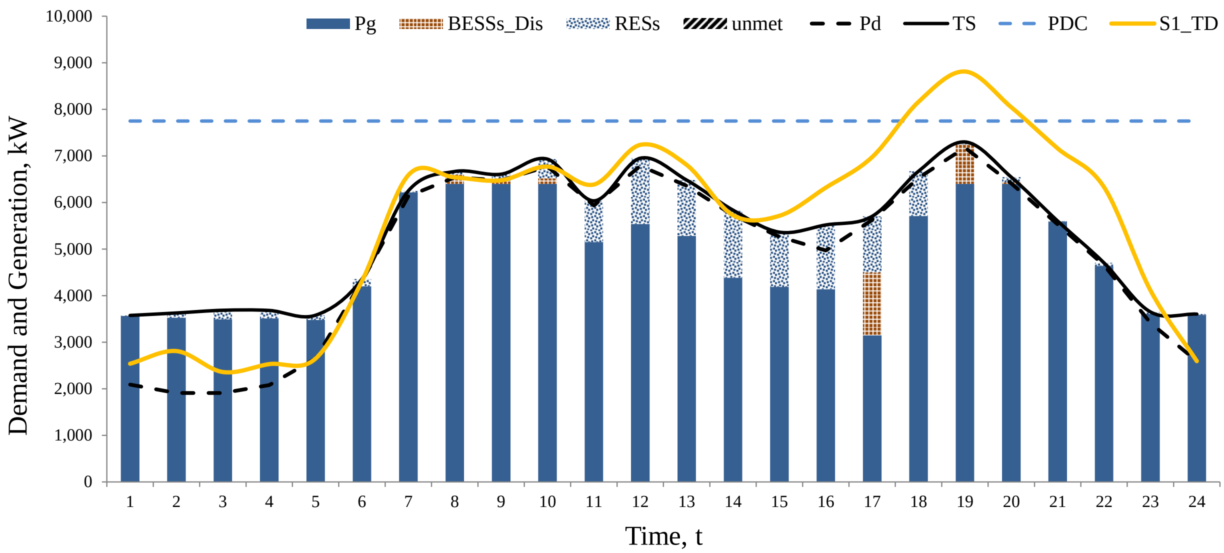


Figure 3.13: The 24-Hour Energy Schedule for Scenario S4

In Scenario S5, the MGO optimally schedules the charging load of PEVs taking into account all the system limits and assumes that customers behave rationally to minimize their charging cost. As observed in Figure 3.15, the PEVs charging periods are not similar to those in Scenarios S3 and S4. The MGO sends a control signal to PEVs owners to start charging while ensuring that the total system demand satisfies (3.26). It is noted that PEVs start charging at hour 21 and the charging lasts for 5 hours, until the batteries are fully charged at one o'clock in the morning.

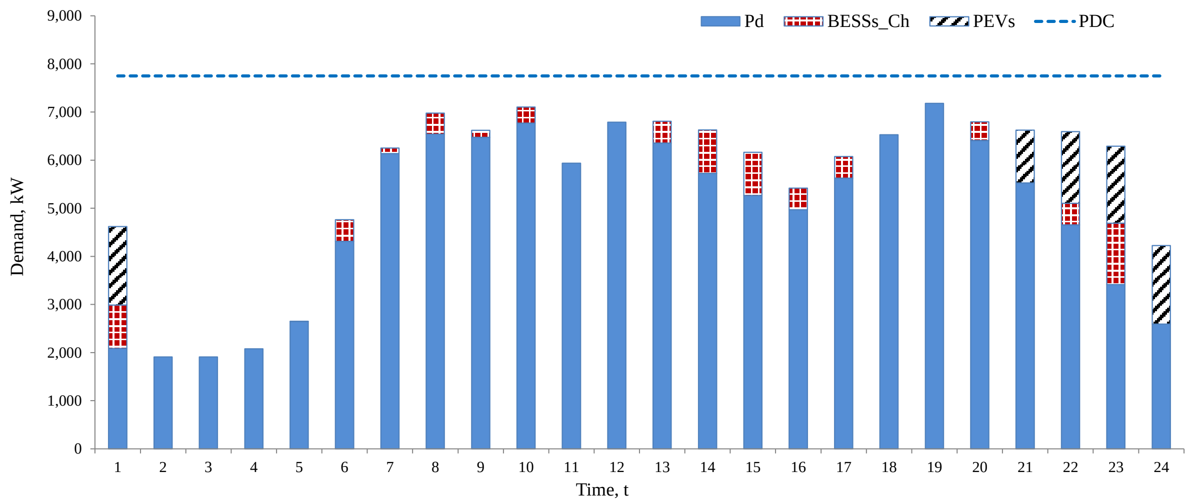


Figure 3.14: THE 24-HOUR DEMAND PROFILE FOR SCENARIO S5

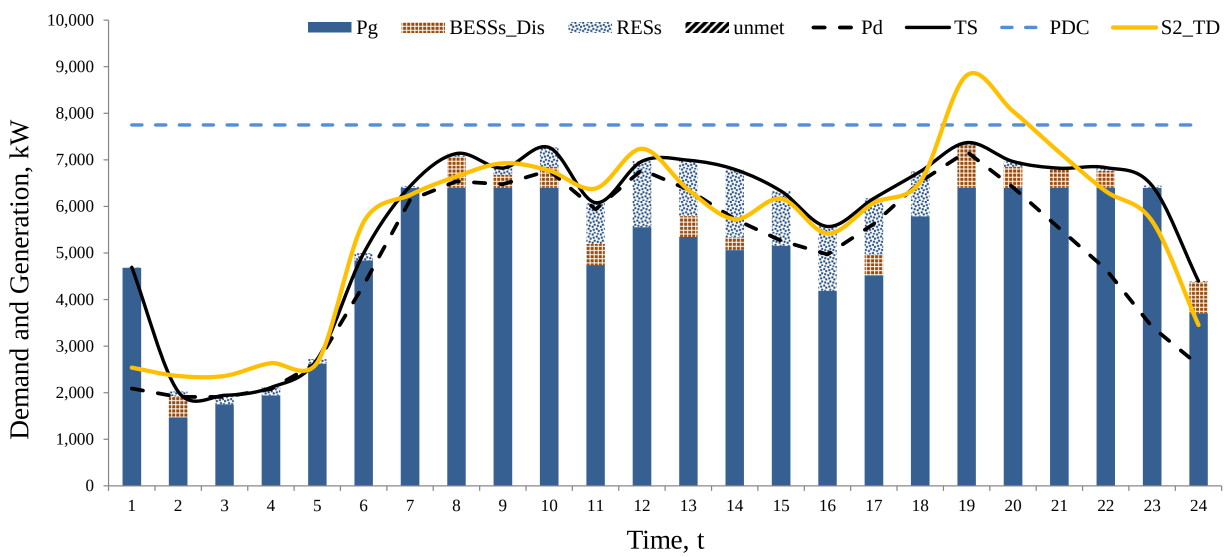


Figure 3.15: THE 24-HOUR ENERGY SCHEDULE FOR SCENARIO S5

Since the MGO imposes the PDC (3.26) and smart charging is applied, PEV charging periods are distributed over the available hours in such a manner that the total microgrid demand including the charging load can be supplied by generation resources. The total supply during the PEV charging hours increases and is close to the original peak demand but still within the limits. Furthermore, the total demand profile (Figure 3.14) becomes fairly flat as the some of the demand activities are shifted from peak to off-peak hours as much as possible.

From a comparison of the results obtained in Scenarios S2 and S5, Table 3.7 shows that if the MGO considers smart charging of PEVs, the smart charging will result in considerable decrease in diesel dispatch. The total charging energy of the BESSs in S5 (smart charging) is 7,646 kWh which is 1221 kWh less than the energy consumed in S2 (uncoordinated charging). Furthermore, The total discharging energy of the BESSs in Scenario S5 is equal to 6,279 kWh, which is significantly lower than the uncoordinated charging Scenario (S5) owing to the reduced peak demand by smartly scheduling the PEVs charging.

Table 3.7: Energy Dispatch Comparison Between Scenario S2 and Scenario S5

| | **Diesel Generation** | **BESSs Charging** | **BESSs Discharging** | **Unmet Energy** |
|---|---|---|---|---|
| | kWh | kWh | kWh | kWh |
| **S2** | 118,939 | 8,867 | 7,718 | 2,613 |
| **S5** | 115,885 | 7,646 | 6,279 | 0 |
| **Energy Saving** | 3,054 | 1,221 | 1,439 | – |

It can be seen from Table 3.7 that the total energy savings accrued from coordinated charging of PEVs (S5) for the day is 5,714 kWh, which is significantly high, and this can be projected to be 2,086 MWh annually.

### 3.5.3 Case 2: Impact of DR

The demand is influenced by control signals from the MGO and the quantity of demand shifted depends on the objective function and other operating constraints. The effect of DR on the operation of the isolated microgrid is presented alongside a comparative study of Case-1, Scenario S2.

Table 3.8 presents the study results considering various percentages of shiftable demand $B_{up}$ and $B_{dn}$ of (3.21) and (3.22), respectively. Initially, when the MGO does not apply the DR option (Scenario S2), there is 2,613 kWh of unmet energy over 24 hours which increases the total cost for the MGO to be 38,882 \$/day. When the DR option is introduced with a transaction cost for the shifted demand, and $B_{up}$ and $B_{dn}$ is set to 6% both the unmet energy and the total cost for MGO reduces. The charging periods of PEVs stays the same as in Scenario S2. Since the PEV charging periods are concentrated at hours 19−23, the system peak demand exceeds the PDC and the MGO has an unmet energy of 1,470 kWh. The total reduction in the unmet energy over the scheduling period of 24-hours is 1,143 kWh comapred to Scenario S2, which corresponds to 6% of the shiftable demand (1,470 kWh). It should be mentioned that when the demand profile is exposed to the DR (S6), there is a significant cost saving of \$685 which also corresponds to 6% of the shiftable demand, as shown in the Table 3.8.

Table 3.8: Summary of Various Percentages of Shiftable Demand

| | | S2 | Scenario S6 With Different % of DR | | | | | | | | |
|---|---|---|---|---|---|---|---|---|---|---|---|
| | | No DR | **6%** | **8%** | **10%** | **12%** | **14%** | **15%** | **16%** | **18%** | **19%** |
| **Total Cost** | \$/day | 38,882 | 38,196 | 38,080 | 37,756 | 37,575 | 37,491 | 37,192 | 36,993 | 37,358 | 37,511 |
| **Diesel Generators Cost** | \$/day | 31,601 | 31,927 | 32,190 | 32,346 | 32,335 | 32,598 | 32,517 | 32,323 | 32,564 | 32,718 |
| **PEVs Charging Cost** | \$/day | 559 | 559 | 559 | 559 | 559 | 559 | 559 | 559 | 559 | 559 |
| **Unmet Energy Cost** | \$/day | 7,840 | 4,409 | 3,264 | 2,202 | 1,031 | 270 | 0 | 0 | 0 | 0 |
| **DR Cost** | \$/day | 0 | 2,420 | 3,184 | 3,767 | 4,769 | 5,182 | 5,234 | 5,229 | 5,352 | 5,352 |
| **MGO Cost Saving** | \$/day | – | 685 | 803 | 1,126 | 1306 | 1,391 | 1,742 | 1,889 | 1,525 | 1,371 |
| **Unmet Energy** | kWh | 2,613 | 1,470 | 1,088 | 734 | 344 | 90 | 0 | 0 | 0 | 0 |
| **Shifted Energy** | kWh | 0 | 1,210 | 1,592 | 1,884 | 2,385 | 2,591 | 2,617 | 2,615 | 2,676 | 2,676 |

To better demonstrate the impact of DR, various percentage values of $B_{up}$ and $B_{dn}$ are considered, and it is noted how the total cost for the MGO and the unmet energy changes under smart charging of PEVs. As the MGO increases the value of $B_{up}$ and $B_{dn}$, which quantify the percentage of shiftable load at each hour, the cost savings increases because of the significant reduction in unmet energy.

It is to be noted from Table 3.8 that for $B_{up}$ and $B_{dn}$ of 15% or higher, there is no unmet energy. Figure 3.16 shows that when MGO sets the value of $B_{up}$ and $B_{dn}$ to be 16%, it appears to be the optimal choice for selecting the amount of the shiftable demand.

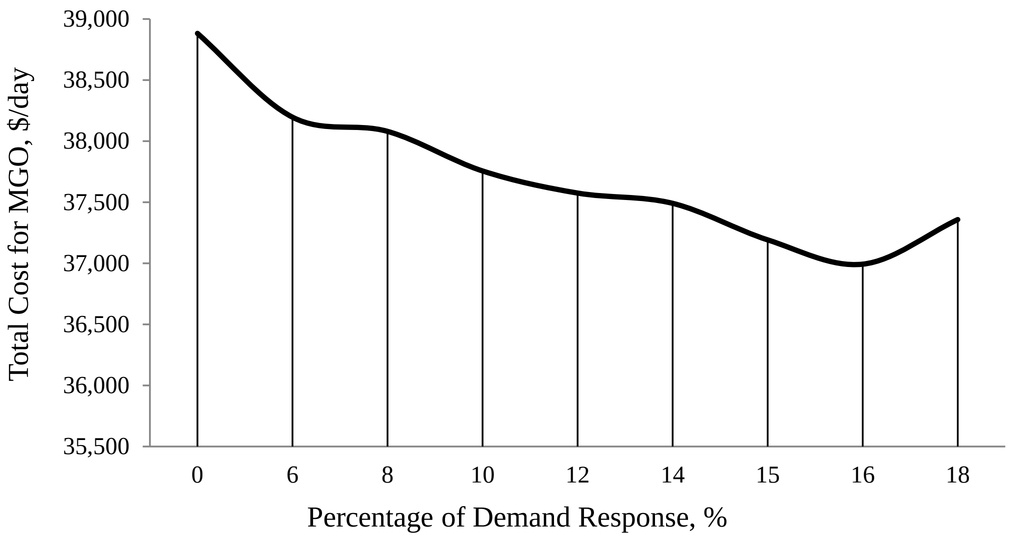


Figure 3.16: Impact of DR on the Total Cost for the MGO

As can be seen in Figure 3.17, PEVs start charging at hour 19 and the charging lasts for five hours, until the batteries are fully charged. The charging load profile coincides with the peak demand hours. The MGO has adopted DR which shifts some of the selected activities from peak to off-peak hours, as shown in Figure 3.18, in order to make room for the charging of PEVs. Basically, the total system demand which includes the variable demand ($dp_{i,t}$), the charging of PEVs ($P_{i,t}^{PEV}$), and the charging of BESSs ($P_{i,t}^{BESS,ch}$). Despite the fact that constraint (3.26), PDC, is not imposed on this case, the total system demand is clearly below the PDC as shown in Figure 3.17. This case results in a fairly flat load profile, but with the creating of a new peak as a result of the PEV charging loads. It is clear that applying 16% of the DR has the benefit of arriving at an optimal solution that does not leave the MGO with unmet energy; hence, there is no need to install new DGs or shed some load.

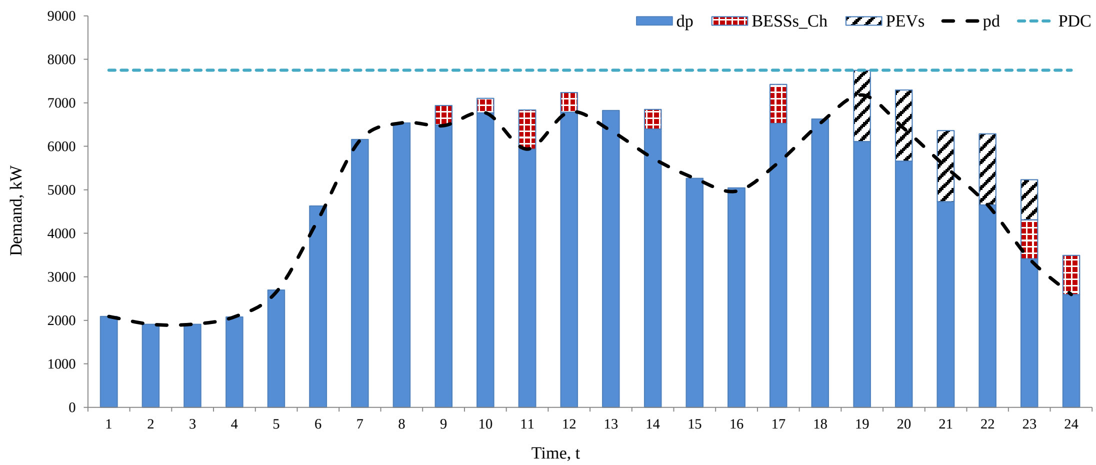


Figure 3.17: Total Demand Profiles with 16% DR

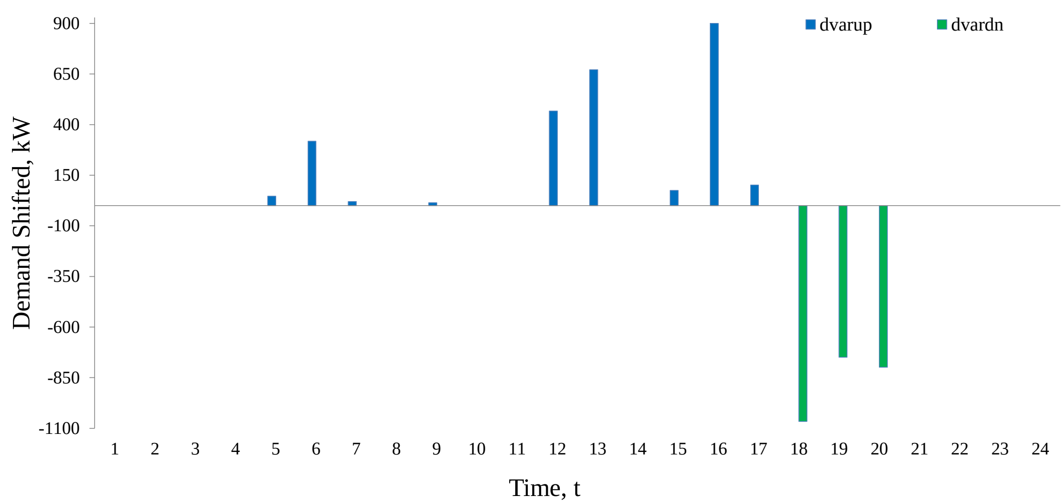


Figure 3.18: Shiftable Demand with 16% DR

Table 3.9 shows that the MGO can have a total savings of $1,889, for this specific day under study. The cost saving is achieved when the MGO introduced DR options and the PEVs charging happens at the peak hours. The MGO ends up with a projected yearly savings of $689,485.

Table 3.9: Energy Dispatch Cost Comparison of Various Scenarios

| | **Diesel Generation** | **Unmet Energy** | **PEV Cost** | **Shifted Energy** | **Total Cost** | **Cost Saving** |
|---|---|---|---|---|---|---|
| | $/day | $/day | $/day | $/day | $/day | $/day |
| **S2** | 31,601 | 7,840 | 559 | 0 | 38,882 | – |
| **S5** | 32,834 | 0 | 559 | 0 | 31,834 | 7,048 |
| **S6** | 32,323 | 0 | 559 | 5,229 | 36,993 | 1,889 |

It is also noted from Table 3.9 that when the MGO considers Scenario S5, a significant cost saving can be achieved to the order of $7,048, for this specific day under study; hence, the yearly savings when Scenario S5 applied is $2,572,520. This saving is significant considering the scope and size of isolated microgrid. Therefore, it is recommended that MGO uses smart charging, and in case there is a charging at the peak hours the DR option is advantageous to the MGO and the customers.

## 3.6 Summary and Conclusions

This chapter has presented a comprehensive mathematical model applied on a modified CIGRE microgrid benchmark considering six different scenarios to address the impact of PEVs and DR on the energy scheduling. This mathematical model efficiently incorporates and manages various supply components, such as diesel generators, BESSs, wind turbines, and solar PV panels, and manages to coordinate the charging load of PEVs in the presence of DR. The proposed model is also applied to investigate the impact of uncontrolled charging *vis-à-vis* smart charging of PEVs and DR. The results successfully demonstrate the effects of PEV charging loads on an isolated microgrid with and without DR.

The simulation results in this chapter indicates that the smart charging of PEVs can effectively diminish the energy management problems, increase the saving of the MGO, and decrease the power losses. Also, it can be concluded from the studied scenarios of Case-1 that uncontrolled charging of PEVs can result in violation of microgrid operations constraints and induce load spikes that cannot be served. In contrast, smart charging is shown to be more efficient in scheduling the PEV charging loads at appropriate hours and keeping the system within its limits for different objective functions. Furthermore, the simulation results in Case-2 shows that the DR options can help the MGO effectively eliminate the introduced unmet energy caused by charging of PEVs at peak hours. In the final analysis, smart charging of PEVs is recommended for both the MGO and the owners of PEVs in the context of isolated microgrids, and also DR would benefit the MGO if the PEVs charging occurs at peak hours.

# Chapter 4

# A Stochastic Optimization Model For Energy Management and Smart Charging of PEVs

## 4.1 Introduction

In Chapter 3, the impact of uncoordinated and smart PEV charging on isolated microgrid in the presence of DR is investigated in detail, considering various objective functions to reflect the perspective of the MGO and PEV owners. As the load profile of the microgrid varies over time depending on different factors, such as temperature and end-user behavior, it is important to consider the randomness of energy consumption. Also, with the increased penetration of RESs such as wind and solar, generally assuming to be an essential part of microgrid systems, there are some challenges to be dealt with, such as the inherent intermittency and variability of these resources. This will make the isolated microgrid operation more complicated and the impact of uncertainties on system operation needs to be investigated.

In this chapter, a novel stochastic short-term operations model of an isolated microgrid considering DR and PEV charging loads is developed. The proposed stochastic model considers the impact of wind and solar generation output variability as well as the effect of uncertain energy consumption patterns of customers. Moreover, the SOC of the PEV battery at the start of charging is not the same for all the customers, and accordingly the effect of uncertain initial SOC of PEV battery is considered in the stochastic model.

## 4.2 Handling Uncertainty

In order to handle the uncertainty in the proposed stochastic optimization model, the forecast data $X_f(t)$ is typically represented by two components, an expected value of the data $X_e(t)$ and a forecast error $e_x(t)$ as shown below:

$$X_f(t) = X_e(t) + e_x(t) \tag{4.1}$$

The forecast error follows a continuous probabilistic distribution function which can be converted into a discrete distribution and consequently formulate a set of scenarios. It should be noted that the number of scenarios grows exponentially with system variables and the scheduling horizon. A common way to represent the forecast error is by utilizing a normal probability distribution function. Accordion to [65, 66], the actual demand can vary from forecast load within a small range and the deviation of load is between ±1% and ±7%. It should be noted that the forecast distribution can be biased either positively or negatively, or symmetric.

The multi-scenario approach used in [26] to handle uncertainties is modified and applied in this thesis. Typically, the number of scenarios created is the multiplication of each set of scenarios; in this thesis, load, wind, solar, and the initial SOC of PEV battery have a set of three scenarios each. So, the total number of scenarios is calculated as follows:

$$S = n \times m \times q \times f \tag{4.2}$$

$S$ is the total number of scenarios created, which is in this thesis, is 81 scenarios; and the $n$, $m$, $q$, and $f$ represent the discrete sets sizes for load, wind, solar, and the initial SOC of the PEV battery, respectively.

The discrete probability distribution sets of the forcasted error for load ($\delta_L$), wind ($\delta_{PW}$), solar ($\delta_{PV}$), and the initial SOC of PEV battery ($\delta_{PEV}$) are represented as follows:

$$\delta_L = \left\{(e_L^1, \rho_L^1), (e_L^2, \rho_L^2), ........., (e_L^n, \rho_L^n)\right\} \tag{4.3}$$

$$\delta_{PW} = \left\{(e_{PW}^1, \rho_{PW}^1), (e_{PW}^2, \rho_{PW}^2), ........., (e_{PW}^m, \rho_{PW}^m)\right\} \tag{4.4}$$

$$\delta_{PV} = \left\{(e_{PV}^1, \rho_{PV}^1), (e_{PV}^2, \rho_{PV}^2), ........., (e_{PV}^q, \rho_{PV}^q)\right\} \tag{4.5}$$

$$\delta_{PEV} = \left\{(e_{PEV}^1, \rho_{PEV}^1), (e_{PEV}^2, \rho_{PEV}^2), ........., (e_{PEV}^f, \rho_{PEV}^f)\right\} \tag{4.6}$$

The error in each element of a a set, for example $e_L^1$ is associated with the probability of that error, $\rho_L^1$. It should be noted that the summation of all the error states probabilities equals to unity, *i.e.*,

$$\sum_{a=1}^{n} \rho_L^a = \sum_{a=1}^{m} \rho_{PW}^a = \sum_{a=1}^{q} \rho_{PV}^a = \sum_{a=1}^{f} \rho_{PEV}^a = 1 \tag{4.7}$$

where $a$ is the state of the load, wind, solar, and the initial SOC of the PEV battery for the forecasting error.

When solving a stochastic optimization problem, the objective function will be multiplied by the joint probability of each scenario created, and the summation of joint probabilities for all scenarios must be equal to unity.

$$\rho^s = \rho_L^s \, \rho_{PW}^s \, \rho_{PV}^s \, \rho_{PEV}^s \tag{4.8}$$

$$\sum_{s=1}^{S} \rho^s = 1 \tag{4.9}$$

## 4.3 Mathematical Model Formulation Under Uncertainty

This section presents a stochastic mathematical model formulation for an isolated microgrid for short term operation. The model discussed in Chapter 3, and is modified in this chapter to capture the range of uncertainties in the load, wind and solar generation, and the initial SOC of PEV batteries.

### 4.3.1 Objective Functions

Two objective functions developed in Section 3.2 are modified in order to incorporate the uncertainties of the load, wind, solar, and the initial SOC of the PEV battery, and consequently study the impact of smart charging of PEVs loads on the isolated microgrid operation, taking into account the DR option.

*Minimize the Total Expected Cost of Operation*

The total expected operational cost of the isolated microgrid over a period of 24-hours, is given below:

$$E[J_1] = \sum_{s=1}^{S} \rho_s \Bigg[ \sum_{i=1}^{N} \sum_{t=1}^{T} \left( a_i Pg_{i,t,s}^2 + b_i Pg_{i,t,s} + c_i \right) + \sum_{i=1}^{N} \sum_{t=1}^{T} dVar_{i,t,s}^{up}\, Co_t^{DR} + \sum_{i=1}^{N} \sum_{t=1}^{T} P_{i,t,s}^{unmet}\, Co_t^{unmet} \Bigg] \quad (4.10)$$

The first term of (4.10) represents the expected operating cost of diesel generators at each bus, hour, and scenario, and the second term denotes the expected demand shifting cost at a bus, hour, and scenario through payment made to the customer. The expected cost of unmet energy, if the demand cannot be served at each bus, hour, and scenario by the available resources is represented by the third term. It should be noted that the production cost from wind and solar generation systems, and the BESS is assumed to be negligible since the MGO operates and owns these systems. The coeffcients $Co_t^{DR}$ and $Co_t^{unmet}$ represent the cost associated with shifting the demand and the cost of unmet energy, respectively.

*Minimize the Total Expected Charging Cost of PEVs*

This objective seeks to determine the optimal operating decision while considering the customers' prespective of minmizing the charging cost, assuming that customers behave rationally.

$$E[J_2] = \sum_{s=1}^{S} \rho_s \left[ \sum_{t=1}^{M} P_{ev,t,s}^{PEV} \, Co_t^{ch} \right] \tag{4.11}$$

In (4.11), $Co_t^{ch}$ is the tariff rate charged by the MGO from PEV customers.

### 4.3.2 System Operating Constraints

The stochastic short-term operations model of the isolated microgrid includes a set of constraints. These constraints were introduced previously in Chapter 3, but for the sake of continuity and completeness are briefly discussed here. Note that all the variables associated with the constraints now include the index for scenarios, S, as well.

## DG Operating limits

The active and reactive power generation from DG units are constrained by their upper and lower limits, as given below:

$$Pg_{min} \leq Pg_{i,t,s} \leq Pg_{max} \qquad \forall\, s \in S, i \in N, t \in T \tag{4.12}$$

$$Qg_{min} \leq Qg_{i,t,s} \leq Qg_{max} \qquad \forall\, s \in S, i \in N, t \in T \tag{4.13}$$

### BESS Constraints

All constraints associated with the BESSs are modified to adopt to the proposed stochastic optimization framework:

$$P^{BESS,ch}_{i,t,s} \leq P^{BESS}_{max} X^{ch}_{i,t,s} \qquad \forall s \in S, i \in N, t \in T \tag{4.14}$$

$$P^{BESS,dis}_{i,t,s} \leq P^{BESS}_{max} X^{dis}_{i,t,s} \qquad \forall s \in S, i \in N, t \in T \tag{4.15}$$

Equations (4.14) and (4.14) constrain the power that is either absorbed or injected by each BESS unit, and this power does not exceed the maximum limits.

$$E^{BESS}_{i,t+1,s} = E^{BESS}_{i,t,s} + P^{BESS,ch}_{i,t,s} \eta^{in} \Delta h \qquad \forall s \in S, i \in N, t \in T \tag{4.16}$$

$$E^{BESS}_{i,t+1,s} = E^{BESS}_{i,t,s} - \frac{P^{BESS,dis}_{i,t,s}}{\eta^{out}} \Delta h \qquad \forall s \in S, i \in N, t \in T \tag{4.17}$$

Equations (4.16) and (4.17) represent the energy relationship in each BESS taking into account the energy consumed/injected by the BESS during charging/discharging process, respectively.

$$E^{BESS}_{min} \leq E^{BESS}_{i,t,s} \leq E^{BESS}_{max} \qquad \forall s \in S, i \in N, t \in T \tag{4.18}$$

The stored energy in the BESS, $E^{BESS}_{i,t,s}$, is restricted between the maximum and minimum values, shown in (4.18).

$$E^{BESS}_{i,t,s}\Big|_{t=0} = E^{BESS}_{S} \qquad \forall s \in S, i \in N, t \in T \tag{4.19}$$

$$E^{BESS}_{i,t,s}\Big|_{t=T} = E^{BESS}_{F} \qquad \forall s \in S, i \in N, t \in T \tag{4.20}$$

The stored energy in the BESS has specified initial and final values which represents the available energy at $t = 0$ and $t = T$ as shown in (4.19) and (4.20).

Finally, the coordination between the charging and discharging states to ensure appropriate decision variables are obtained, and that the batteries do not charge and discharge simultaneously, are ensured by the following constraints:

$$X^{dis}_{i,t,s} + X^{ch}_{i,t,s} \leq 1 \qquad \forall\, s \in S, i \in N, t \in T \tag{4.21}$$

## Constraints on PEV Charging Operation

In order to appropriately model the charging load of the PEVs under uncertainty, the introduced set of constraints in Section 3.2 are re-modeled in this chapter to consider the stochastic nature of the initial SOC of the PEV battery.

The constraints linked with the battery energy balance of the PEVs, and the limit on power drawn from the outlet, are presented below, respectively:

$$E^{PEV}_{ev,t+1,s} = E^{PEV}_{ev,t,s} + \eta^{ch}\, P^{PEV}_{ev,t,s}\, \Delta h \qquad \forall\, s \in S, ev \in N, t \in T \tag{4.22}$$

$$P^{PEV}_{ev,t,s} \leq P^{PEV}_{max} \qquad \forall\, s \in S, ev \in N, t \in T \tag{4.23}$$

The energy stored in the PEV battery is constrained by upper and lower limits of the battery storage considering practical aspects of the charging and battery characteristic, as given below:

$$E^{PEV}_{min} \leq E^{PEV}_{ev,t,s} \leq E^{PEV}_{max} \qquad \forall\, s \in S, ev \in N, t \in T \tag{4.24}$$

The preferred plug-out time of the PEV batteries is given by the following:

$$E^{PEV}_{ev,t,s} = E^{PEV}_{max} \qquad \forall\, s \in S, ev \in N, t = h_{po,t,s} \tag{4.25}$$

It should be noted that when a PEV returns to the garage, the remaining energy in the battery of PEV varies from one customer to another. The stochastic nature of the initial SOC of the PEV battery is considered, as per the following constraint:

$$E_{ev,t,s}^{BESS}\Big|_{t=0} = E_{s}^{BESS} \qquad \forall\, s \in S, ev \in N, t \in T \tag{4.26}$$

## DR Constraints

The DR constraints introduced in Chapter 3 are also modify, the variable demand $dP_{i,t,s}$ is redefined as the demand at each bus, hour, and scenario, and can be equal, more, or less than the base demand.

$$dP_{i,t,s} = Pd_{i,t,s} + dVar_{i,t,s}^{up} - dVar_{i,t,s}^{dn} \qquad \forall\, s \in S, i \in N, t \in T \tag{4.27}$$

This variable demand $dP_{i,t,s}$ in (4.27) is constrained by the following constraints:

$$\sum_{i}^{N}\sum_{t}^{T} dVar_{i,t,s}^{up} = \sum_{i}^{N}\sum_{t}^{T} dVar_{i,t,s}^{dn} \qquad \forall\, s \in S, i \in N, t \in T \tag{4.28}$$

The upward and downward demand variation are limited by the following constraints:

$$0 \leq dVar_{i,t,s}^{up} \leq B_{up} \cdot Pd_{i,t,s} \qquad \forall\, s \in S, i \in N, t \in T \tag{4.29}$$

$$0 \leq dVar_{i,t,s}^{dn} \leq B_{dn} \cdot Pd_{i,t,s} \qquad \forall\, s \in S, i \in N, t \in T \tag{4.30}$$

## Demand-Supply Constraints

The demand-supply balance constraints of the isolated microgrid is modified to adopt to the stochastic optimization model scenarios, as follows:

$$\begin{aligned} Pg_{i,t,s} + PW_{i,t,s} + PV_{i,t,s} + P_{i,t,s}^{BESS,dis} + P_{i,t,s}^{unmet} - P_{ev,t,s}^{PEV} - P_{i,t,s}^{BESS,ch} - dP_{i,t,s} \\ = V_{i,t,s}\sum_{j=1}^{N} V_{j,t,s}\left[G_{ij}\cos(\theta_{ij}) + B_{ij}\sin(\theta_{ij})\right] \end{aligned} \tag{4.31}$$

$$Qg_{i,t,s} - Qd_{i,t,s} = V_{i,t,s} \sum_{j=1}^{N} V_{j,t,s} \left[ G_{ij} \sin(\theta_{ij}) - B_{ij} \cos(\theta_{ij}) \right] \tag{4.32}$$

The remaining model constraints are similar to the ones presented in Section 3.2, except that the index for scenarios are introduced in there, whenever appropriate.

## 4.4 System Under Study

The isolated microgrid of CIGRE benchmark that is adopted in Chapter 3 is also considered in this chapter to carry out the uncertainty analysis. A total of 81 scenarios are considered that include 3 different discrete probability distributions of the forecasting errors of the load, wind, solar, and the initial SOC of the PEV battery. All discrete probability distribution functions are shown in Table 4.1 which are adopted in this chapter [26].

Table 4.1: Discrete Probability Distribution of Wind and Solar Resources, Load, and PEV

| $SOC_{ev}$ | | Wind | | Load | | Solar | |
|---|---|---|---|---|---|---|---|
| % of deviation | Probability | % of deviation | Probability | % of deviation | Probability | % of deviation | Probability |
| $e_{PEV}$ | $\rho_{PEV}$ | $e_{PW}$ | $\rho_{PW}$ | $e_L$ | $\rho_L$ | $e_{PV}$ | $\rho_{PV}$ |
| − 20% | 0.2 | − 5 | 0.2 | − 6 | 0.1 | − 5 | 0.15 |
| 0 | 0.6 | 0 | 0.6 | 0 | 0.8 | 0 | 0.7 |
| + 20 | 0.2 | + 5 | 0.2 | + 6 | 0.1 | + 5 | 0.15 |

The normal state is defined as the state where the deviation from the forecasted value is zero. Furthermore, the low state is where the deviation from the forecasted value has a negative value whereas the high state is defined when the deviation from the foretasted value has a positive value. Therefore, when the load has a positive deviation, and wind and solar output generation and the initial SOC of the PEV battery have a negative deviation, it is considered to be the worst case scenario. On the other hand, when the wind and solar output generation and the initial SOC of the PEV battery have a positive deviation, and the load has a negative deviation, it is considered to be the best case scenario.

The PEV charging load data, such as the plug-in time, the preferred plug-out time, and the battery capacity of PEV, in this chapter are similar to what are presented in Chapter 3. The only difference in this chapter is that the initial SOC of PEV battery is varied based on different scenarios.

## 4.5 Definition of Cases

In this chapter, the MGO examine the effects of uncertainties on the operational aspects of the isolated microgrid considering smart charging of PEVs and DR options. Four different cases are examined, as described below:

### 4.5.1 Case-1: Neither PEVs nor DR

In this case, neither PEVs nor demand shifting are considered; the stochastic mathematical optimization model developed in Section 4.3 is applied on the modified CIGRE microgrid with an objective of minimizing the total expected cost for the MGO, (4.10). A total of 27 scenarios are considered to study the impact of uncertainties of the load, solar, and wind on the isolated microgrid energy scheduling problem.

### 4.5.2 Case-2: Smart Charging of PEVs

This case examines the impact of smart charging of PEVs on isolated microgrid operation when a total of 81 scenarios are considered to study the impact of uncertainties of the load, solar, wind, and the initial SOC of the PEV battery on the isolated microgrid energy scheduling problem. The two objective functions introduced in (4.10) and (4.11), are used to formulate two sub-cases as follows:

- *Case-2a* : The objective is minimization of $E[J_1]$.
- *Case-2b* : The objective is minimization of $E[J_2]$.

The time required to charge the PEVs is different from one uncertainty scenario to another because the initial SOC of the PEV battery is not the same across scenarios. It is also assumed that the customers are aware of the different costs of charging at peak hours and off-peak hours, as per the TOU price [64].

### 4.5.3 Case-3: Smart Charging of PEVs with Fixed DR

In this Case, the MGO studies the impact of DR while also considering smart charging of PEVs to minimize its total expected operating cost over 24-hours, as given in (4.10), and denoted by *Case-3a*; and that customers seek to minimize their PEV charging cost over 24-hours, as given in (4.11), denoted by *Case-3b*; in both sub-cases, the maximum amount of shiftable microgrid demand $B_{up}$ and $B_{dn}$ is fixed over the 24-hours period at 6% of the demand of the hour (4.29) and (4.30), respectively.

### 4.5.4 Case-4: Smart Charging of PEVs with Optimal DR

The MGO seeks to minimize its total expected operating cost over 24-hours, (4.10) denoted by *Case-4a*; and the customers seek to minimize their PEV charging cost over 24-hours, (4.11) denoted by *Case-4b*. The maximum amount of shiftable microgrid demand $B_{up}$ and $B_{dn}$ are considered to be optimization variables and determined from the model.

## 4.6 Results, Analyses, and Discussions

Since the benchmark test system has a critical load profile, the diesel generators will be committed over all the scheduled time horizon whereas the dispatch of these units will vary from one scenario to another. The value of the load, wind, solar, and the initial SOC of the PEV battery in each scenario is attached to a probability of the likelihood of this scenario. GAMS environment is used to execute, and solve the considered microgrid benchmark CIGRE system [67]. The following paragraphs present results of the four cases defined in the previous section.

### 4.6.1 Case-1: No PEVs, No DR

This case studies the impact of uncertainties (load, solar, and wind) on the isolated microgrid energy scheduling problem. The total expected operating cost for the MGO shown in Table 4.2 is 29,383 \$/day which is slightly higher than the deterministic case (29,278 \$/day) presented in the Chapter 3. The expected total loss is increased as well to reach 2010 kWh whereas in the deterministic case the total loss was 1962 kWh.

Table 4.2: SUMMARY RESULTS OF CASE-1

| Expected DG Cost | Expected PEV Cost | Expected unmet Cost | Expected Total Cost | Expected Total Loss |
|---|---|---|---|---|
| \$/day | \$/day | \$/day | \$/day | kWh |
| 29,383 | – | – | 29,383 | 2,010 |

Since the demand and RES generation are not fixed any more, the BESS units consequently respond to the variation in the demand and the generation, the total expected operating cost for the MGO is thus increased. The results of most favourable scenario (S9), which has the lowest demand and highest generation from wind and solar, and the least favourable scenario (S19), where the demand is high while the RESs generation levels are low, are presented in Table 4.3.

Table 4.3: Summary Results of Different Scenarios in Case-1

| | | **S19** | **S9** |
|---|---|---|---|
| **Total Cost** | $/day | 31,207 | 27,603 |
| **Charging Energy of BESSs** | kWh | 3,932 | 603 |
| **Discharging Energy of BESSs** | kWh | 4,535 | 1,839 |
| **Total Loss** | kWh | 2,261 | 1,772 |
| **Unmet Energy** | kWh | – | – |

### 4.6.2 Case-2: Smart Charging of PEVs

The results obtained in *Case-2a* and *Case-2b* are presented in Table 4.4, which considers 81 different scenarios. It should be noted that when uncertainty is taken into account the isolated microgrid can expect some energy to remain unmet, which is higher in *Case-2b* when the customers seek to minimize their charging cost of the PEVs.

It is noted from Table 4.4 that the MGO suffers in *Case-2a* and *Case-2b* a total expected unmet energy of 10 kWh and 120 kWh for a specific day, respectively, even though it utilizes smart charging to charge the PEVs.

Table 4.4: Summary Results of Case-2

| | Expected DG Cost | Expected PEV Cost | Expected DR Cost | Expected unmet Cost | Expected Total Cost | Expected Total Loss |
|---|---|---|---|---|---|---|
| | $/day | $/day | $/day | $/day | $/day | kWh |
| *Case-2a* | 30,989 | 419 | – | 30 | 30,600 | 2,623 |
| *Case-2b* | 31,766 | 419 | – | 360 | 31,707 | 3,893 |

### 4.6.3 Case-3: Smart Charging of PEVs with Fixed DR

In this case, the adoption of DR helps the MGO by shifting the demand from peak to off-peak hours, and hence reducing the total expected operating cost and the expected unmet energy as compared to Case-2.

It is noted from Table 4.5 that in *Case-3a*, the total expected operating cost is reduced to 29,303 $/day compared to the cost in *Case-2a* of 30,600 $/day. Moreover, it is noted from Table 4.5 that in *Case-3b*, the total expected operating cost is reduced to 31,651 $/day compared to the cost in *Case-2b* of 31,707 $/day. The total expected loss is reduced as well to 2,422 kWh and 3,765 kWh for a specific day in *Case-3a* and *Case-3b*, respectively, when DR is considered compared to *Case-2a* and *Case-2b*.

Table 4.5: Summary Results of Case-3

| | Expected DG Cost | Expected PEV Cost | Expected DR Cost | Expected unmet Cost | Expected Total Cost | Expected Total Loss |
|---|---|---|---|---|---|---|
| | $/day | $/day | $/day | $/day | $/day | kWh |
| *Case-3a* | 29,495 | 419 | 204 | 23 | 29,303 | 2,422 |
| *Case-3b* | 31,540 | 419 | 320 | 210 | 31,651 | 3,765 |

In *Case-3a*, the expected total saving cost for the MGO is 1,297 $/day when demand shifting is applied, while the total expected loss is reduced by 201 kWh for a specific day compared to *Case-2a*.

It should be noted that the amount of DR allowed in this case (6% of the demand) is not enough to eliminate the total expected unmet energy, but it helps decreasing the expected unmet energy and hence the total expected operating cost for the MGO.

### 4.6.4 Case-4: Smart Charging of PEVs with Optimal DR

As seen in Table 4.6, the MGO is now able to provide enough generation to meet all the demand when implementing the DR, with $B_{up}$ and $B_{dn}$ being chosen optimally by the model. The optimal values of $B_{up}$ and $B_{dn}$ are obtained as 0.19 and 0.29 for for *Case-4a* and *Case-4b*, respectively. It can be noted from Table 4.6 that the isolated microgrid is no longer has an expected unemet energy since the MGO sets the value of the variable $B_{up}$ / $B_{dn}$ to be 0.19 for *Case-4a* and 0.29 for *Case-4b* .

Table 4.6: SUMMARY RESULTS OF CASE-4

| | Expected DG Cost | Expected PEV Cost | Expected DR Cost | Expected unmet Cost | Expected Total Cost | Expected Total Loss |
|---|---|---|---|---|---|---|
| | \$/day | \$/day | \$/day | \$/day | \$/day | kWh |
| *Case-4a* | 29,604 | 419 | 51 | – | 29,236 | 2,358 |
| *Case-4b* | 31,520 | 419 | 109 | – | 31,210 | 3,681 |

When the maximum amount of shiftable microgrid demand $B_{up}$ and $B_{dn}$ is optimally determined, the total expected saving cost for the MGO in *Case-4a* is 1,364 and 67 \$/day compared to *Case-2a* and *Case-3a*, respectively. Furthermore, the total expected loss is decreased in *Case-4b* by 212 kWh and 84 kWh compared to *Case-2b* and *Case-3b*, respectively

## 4.7 Summary and Conclusions

This chapter deals with short term energy management of an isolated microgrid considering uncertainties. Smart charging of PEVs and the presence of DR are taken into account in a stochastic operation framework modeling. The uncertain parameters considered are load, the output generation of wind and PV, and the initial SOC of the PEV battery. The effect of PEV smart charging on the generation scheduling of isolated microgrid is examined. The impact of fixed and optimal DR ($B_{up}$ / $B_{dn}$) on the energy supply balance of the isolated microgrid has been highlighted.

# Chapter 5

# Conclusions and Future Work

## 5.1 Summary

Energy management in isolated microgrids is crucial as they have a limited generation capacity, some of which are renewable based, and hence intermittent. PEVs are expected to penetrate in the system and hence expected to have an impact on the operation of isolated microgrids too. In order to manage the increase in demand due to the charging of PEVs, the smart charging is a very attractive solution that can significantly improve the operation of the isolated microgrid. Along with smart charging, the DR options have the ability to shift and reduce the consumption of customers from peak to off-peak hours, which make the operation of the isolated microgrid more reliable and efficient.

Chapter 1 presents the motivation behind this research, and it is followed by a literature review of related works addressing the energy management in isolated microgrids, the PEV charging approaches and their impact on the operation of isolated microgrids, and the integration and effect of DR. This chapter lays out the research objectives of this thesis as well.

Chapter 2 presents background review on the subjects, the tools, and the models, that correlate with the the research objectives of this thesis. An overview on smart grid and microgrids is discussed. The essential components of the microgrid, such as BESS, wind, and solar energy resources, are discussed. This chapter also reviews several types of EVs that exists in the market, and highlights various charging levels of EVs. The background review also examines the significant contributions of DSM programs such as DR on the operation of the microgrids. The uncertainty analysis techniques that are applied on various forecasting data have been discussed.

A comprehensive mathematical optimization model for short-term operation of the isolated microgrid is proposed in Chapter 3. This model is used to determine an optimal energy management solution combining generation from different resources such as diesel generators, wind turbines, solar panels, and BESSs, and at the same time utilizing smart charging to coordinate the PEVs. The model also incorporates DR options. Results of several cases and scenarios using the proposed model are evaluated, to obtain insights into the effect of smart charging *vis-à-vis* uncoordinated charging accompanied by DR options. Variety of cases and scenarios are carried out on the modified CIGRE isolated microgrid benchmark, and modeled in GAMS environment.

Chapter 4 presents a novel stochastic optimization model for energy management and smart charging of PEVs in short-term operation of the isolated microgrid considering fixed and optimal DR options. The proposed stochastic optimization model studies the impact of wind and solar generation output variability as well as the effect of uncertain energy consumption patterns of customers; and also the stochastic nature of the SOC of the PEV battery at the start of charging. This chapter also examines the effect of smart charging of PEVs along with fixed and optimal values of DR on the operation of isolated microgrid.

## 5.2 Contributions

The main contributions of this thesis are summarized as follows:

- A comprehensive mathematical optimization model for short-term energy management of isolated microgrids is developed to examine the impact of uncontrolled and controlled (smart) PEV charging. Diesel generators, BESS devices, PV panels and wind turbines are considered for the studies.

- A detailed model of DR option, which provides significant flexibility in the operation of the isolated microgrids, as the isolated microgrids have limited generation capacity, by altering the demand and introducing an elasticity effect, is presented to mitigate the energy management problems and make the system more reliable and efficient.

- The inherent intermittency and variability of solar and wind output generation along with the random energy consumption by customers and the initial SOC of the PEV battery are examined utilizing a novel stochastic optimization model. The proposed problem formulation minimizes the expected operational cost of the isolated microgrid and the expected PEV charging cost by smartly coordinating the charging of PEV, utilizing two different model of DR, and dispatching energy output from various source of generation.

## 5.3 Future Work

Based on the research presented in this thesis, possible future research can be conducted, some ideas presented below:

- The proposed model presented in this thesis could be extended by applying model predictive control based technique to achieve a optimal real time energy balance.

- The ancillary services that can be achieved by using the notion of V2G support which basically utilizes the PEVs stored energy in order to supply critical loads at peak hours and improve some of the system security indices.

- The uncertainty and variability associated with of charging and discharging operations of EVs are not considered in this thesis and it can be addressed. There are many parameters of uncertainty that can be taken into account, such as charging time, daily miles driven, *etc*. Various types of EVs also can be tested and different levels of EV charging could be used.

# References


[1] International energy agency (IEA), world energy outlook 2014, novamber 2014. [Online]. Available: http://www.worldenergyoutlook.org/publications/weo-2014/

[2] World wide fund for nature (WWF), greenhouse gas reduction potential of electric vehicles: 2025 outlook report canada, 2012. [Online]. Available: http://awsassets.wwf.ca/downloads/wwf_ev_report_2012.pdf

[3] H. Liang and W. Zhuang, “Stochastic modeling and optimization in a microgrid: A survey,” *Energies*, vol. 7, no. 4, pp. 2027–2050, 2014.

[4] K. Clement-Nyns, E. Haesen, and J. Driesen, “The impact of charging plug-in hybrid electric vehicles on a residential distribution grid,” *IEEE Transactions on Power Systems*, vol. 25, no. 1, pp. 371–380, Feb 2010.

[5] I. Sharma, C. Canizares, and K. Bhattacharya, “Smart charging of PEVs penetrating into residential distribution systems,” *IEEE Transactions on Smart Grid*, vol. 5, no. 3, pp. 1196–1209, May 2014.

[6] C. Canizares, J. Nathwani, K. Bhattacharya, M. Fowler, M. Kazerani, R. Fraser, I. Rowlands, and H. Gabbar, “Towards an ontario action plan for plug-in-electric vehicles (PEVs),” *Waterloo Institute for Sustainable Energy, University of Waterloo*, 2010.

[7] K. Dietrich, J. Latorre, L. Olmos, and A. Ramos, “Demand response in an isolated system with high wind integration,” *IEEE Transactions on Power Systems*, vol. 27, no. 1, pp. 20–29, Feb 2012.

[8] J. Aghaei and M.-I. Alizadeh, "Demand response in smart electricity grids equipped with renewable energy sources: A review," *Renewable and Sustainable Energy Reviews*, vol. 18, pp. 64 – 72, 2013.

[9] Q. Jiang, M. Xue, and G. Geng, "Energy management of microgrid in grid-connected and stand-alone modes," *IEEE Transactions on Power Systems*, vol. 28, no. 3, pp. 3380–3389, Aug 2013.

[10] E. Sortomme and M. El-Sharkawi, "Optimal power flow for a system of microgrids with controllable loads and battery storage," in *Power Systems Conference and Exposition, 2009. PSCE '09. IEEE/PES*, March 2009, pp. 1–5.

[11] S.-J. Ahn, S.-R. Nam, J.-H. Choi, and S.-I. Moon, "Power scheduling of distributed generators for economic and stable operation of a microgrid," *IEEE Transactions on Smart Grid*, vol. 4, no. 1, pp. 398–405, March 2013.

[12] E. Sortomme, M. Hindi, S. MacPherson, and S. Venkata, "Coordinated charging of plug-in hybrid electric vehicles to minimize distribution system losses," *IEEE Transactions on Smart Grid*, vol. 2, no. 1, pp. 198–205, March 2011.

[13] M. Khodayar, L. Wu, and M. Shahidehpour, "Hourly coordination of electric vehicle operation and volatile wind power generation in SCUC," *IEEE Transactions on Smart Grid*, vol. 3, no. 3, pp. 1271–1279, Sept 2012.

[14] S. Derakhshandeh, A. Masoum, S. Deilami, M. Masoum, and M. Hamedani Golshan, "Coordination of generation scheduling with PEVs charging in industrial microgrids," *IEEE Transactions on Power Systems*, vol. 28, no. 3, pp. 3451–3461, Aug 2013.

[15] Q. Gong, S. Midlam-Mohler, V. Marano, and G. Rizzoni, "Study of PEV charging on residential distribution transformer life," *IEEE Transactions on Smart Grid*, vol. 3, no. 1, pp. 404–412, March 2012.

[16] Z. Ma, D. Callaway, and I. Hiskens, "Decentralized charging control of large populations of plug-in electric vehicles," *IEEE Transactions on Control Systems Technology*, vol. 21, no. 1, pp. 67–78, Jan 2013.

[17] T. Wu, Q. Yang, Z. Bao, and W. Yan, "Coordinated energy dispatching in microgrid with wind power generation and plug-in electric vehicles," *IEEE Transactions on Smart Grid*, vol. 4, no. 3, pp. 1453–1463, Sept 2013.

[18] Y. Cao, S. Tang, C. Li, P. Zhang, Y. Tan, Z. Zhang, and J. Li, "An optimized EV charging model considering TOU price and SOC curve," *IEEE Transactions on Smart Grid*, vol. 3, no. 1, pp. 388–393, March 2012.

[19] W. Su and M.-Y. Chow, "Performance evaluation of an EDA-based large-scale plug-in hybrid electric vehicle charging algorithm," *IEEE Transactions on Smart Grid*, vol. 3, no. 1, pp. 308–315, March 2012.

[20] S. Shao, M. Pipattanasomporn, and S. Rahman, "Grid integration of electric vehicles and demand response with customer choice," *IEEE Transactions on Smart Grid*, vol. 3, no. 1, pp. 543–550, March 2012.

[21] H. Kumar Nunna and S. Doolla, "Energy management in microgrids using demand response and distributed storage - a multiagent approach," *IEEE Transactions on Power Delivery*, vol. 28, no. 2, pp. 939–947, April 2013.

[22] M. Arriaga, C. Canizares, and M. Kazerani, "Renewable energy alternatives for remote communities in northern ontario, canada," *IEEE Transactions on Sustainable Energy*, vol. 4, no. 3, pp. 661–670, July 2013.

[23] W. Alharbi, "Coordinated operation of distributed energy resources in renewables based microgrids under uncertainties," Master's thesis, University of Waterloo, 2013.

[24] Z. Xu, X. Guan, Q.-S. Jia, J. Wu, D. Wang, and S. Chen, "Performance analysis and comparison on energy storage devices for smart building energy management," *IEEE Transactions on Smart Grid*, vol. 3, no. 4, pp. 2136–2147, Dec 2012.

[25] M. Fathi and H. Bevrani, "Statistical cooperative power dispatching in interconnected microgrids," *IEEE Transactions on Sustainable Energy*, vol. 4, no. 3, pp. 586–593, July 2013.

[26] A. Saber and G. Venayagamoorthy, "Resource scheduling under uncertainty in a smart grid with renewables and plug-in vehicles," *IEEE Systems Journal*, vol. 6, no. 1, pp. 103–109, March 2012.

[27] N. Komninos, E. Philippou, and A. Pitsillides, "Survey in smart grid and smart home security: Issues, challenges and countermeasures," *IEEE Communications Surveys Tutorials*, vol. 16, no. 4, pp. 1933–1954, Fourthquarter 2014.

[28] H. Farhangi, "The path of the smart grid," *IEEE Power and Energy Magazine*, vol. 8, no. 1, pp. 18–28, January 2010.

[29] F. Li, W. Qiao, H. Sun, H. Wan, J. Wang, Y. Xia, Z. Xu, and P. Zhang, "Smart transmission grid: Vision and framework," *IEEE Transactions on Smart Grid*, vol. 1, no. 2, pp. 168–177, Sept 2010.

[30] European technology platform for electricity networks of the future (smartgrids). [Online]. Available: http://http://www.smartgrids.eu/

[31] X. Fang, S. Misra, G. Xue, and D. Yang, "Smart grid the new and improved power grid: A survey," *IEEE Communications Surveys Tutorials*, vol. 14, no. 4, pp. 944–980, Fourth 2012.

[32] J. Vasconcelos, "Survey of regulatory and technological developments concerning smart metering in the european union electricity market," European Univeristy institute , Florence, Tech. Rep. Ploicy paper, RSCAS, January 2008.

[33] Comparison of smart grid with traditional grid, january 2014. [Online]. Available: http://www.epri.com/Pages/Default.aspx

[34] National institute of standards and technology (NIST) framework and roadmap for smart grid interoperability standards, january 2010. [Online]. Available: http://www.nist.gov/publicaffairs/releases/upload/smartgridinteroperabilityfinal.pdf

[35] S. Chowdhury and P. Crossley, *Microgrids and active distribution networks*. The Institution of Engineering and Technology, 2009.

[36] Q. Fu, A. Hamidi, A. Nasiri, V. Bhavaraju, S. Krstic, and P. Theisen, "The role of energy storage in a microgrid concept: Examining the opportunities and promise of microgrids." *IEEE Electrification Magazine*, vol. 1, no. 2, pp. 21–29, Dec 2013.

[37] H. Iwasaki, Y. Fujioka, H. Maejima, S. Nakamura, Y. Kojima, and M. Koshio, "Operational analysis of a microgrid: the hachinohe demonstration project," in *Conference International des Grands Reseaux Electriques (CIGRE), C6-109*, 2008.

[38] European research project microgrids project, january 2015. [Online]. Available: http://www.microgrids.eu

[39] H. Qian, J. Zhang, J.-S. Lai, and W. Yu, "A high-efficiency grid-tie battery energy storage system," *IEEE Transactions on Power Electronics*, vol. 26, no. 3, pp. 886–896, March 2011.

[40] Canadian wind energy association (CANWEA), wind energy: Building a stronger, cleaner and more affordable power system in ontario, Feb, 2015. [Online]. Available: http://canwea.ca/wind-energy/ontario/

[41] Y. Atwa, E. El-Saadany, M. Salama, and R. Seethapathy, "Optimal renewable resources mix for distribution system energy loss minimization," *IEEE Transactions on Power Systems*, vol. 25, no. 1, pp. 360–370, Feb 2010.

[42] Natural resources canada (NRCan), solar photovoltaic energy, january 2015. [Online]. Available: http://www.nrcan.gc.ca/energy/renewables/solar-photovoltaic/7303

[43] A. K. Yadav and S. Chandel, "Tilt angle optimization to maximize incident solar radiation: A review," *Renewable and Sustainable Energy Reviews*, vol. 23, no. 0, pp. 503 – 513, 2013. [Online]. Available: http://www.sciencedirect.com/science/article/pii/S1364032113001299

[44] C. Chan, "The state of the art of electric, hybrid, and fuel cell vehicles," *Proceedings of the IEEE*, vol. 95, no. 4, pp. 704–718, April 2007.

[45] International energy agency (IEA) hybrid and electric vheciles, november 2014. [Online]. Available: http://www.ieahev.org

[46] Vehicle technologies program, energy efficiency and renweable energy, united states deprtment of energy (DOE), october 2011. [Online]. Available: http://www.afdc.energy.gov/pdfs/52723.pdf

[47] National household travel survey oakridge national laborotary, united states department of transportation (ROT), 2001. [Online]. Available: http://nhts.ornl.gov

[48] M. Levesque, D. Q. Xu, G. Joos, and M. Maier, "Co-simulation of PEV coordination schemes over a FiWi smart grid communications infrastructure," in *IECON 2012 - 38th Annual Conference on IEEE Industrial Electronics Society*, Oct 2012, pp. 2901–2906.

[49] S. Deilami, A. Masoum, P. Moses, and M. Masoum, "Real-time coordination of plug-in electric vehicle charging in smart grids to minimize power losses and improve voltage profile," *IEEE Transactions on Smart Grid*, vol. 2, no. 3, pp. 456–467, Sept 2011.

[50] B. Davito, H. Tai, and R. Uhlaner, "The smart grid and the promise of demand-side management."

[51] T. Logenthiran, D. Srinivasan, and T. Z. Shun, "Demand side management in smart grid using heuristic optimization," *IEEE Transactions on Smart Grid*, vol. 3, no. 3, pp. 1244–1252, Sept 2012.

[52] F. Boshell and O. Veloza, "Review of developed demand side management programs including different concepts and their results," in *Transmission and Distribution Conference and Exposition: Latin America, 2008 IEEE/PES*, Aug 2008, pp. 1–7.

[53] M. Goldberg, "Measure twice, cut once," *IEEE Power and Energy Magazine*, vol. 8, no. 3, pp. 46–54, May 2010.

[54] H. Shen and Y. Zhu, "The collaboration between demand response and smart grid," in *Sustainable Power Generation and Supply (SUPERGEN 2012), International Conference on*, Sept 2012, pp. 1–4.

[55] M. H. Albadi and E. El-Saadany, "A summary of demand response in electricity markets," *Electric Power Systems Research*, vol. 78, no. 11, pp. 1989–1996, 2008.

[56] S. Frank, I. Steponavice, and S. Rebennack, "Optimal power flow: a bibliographic survey i," *Energy Systems*, vol. 3, no. 3, pp. 259–289, 2012.

[57] X.-P. Zhang, "Fundamentals of electric power systems," *Restructured Electric Power Systems: Analysis of Electricity Markets with Equilibrium Models*, vol. 43, p. 1, 2010.

[58] Y. Makarov, P. Etingov, J. Ma, Z. Huang, and K. Subbarao, “Incorporating uncertainty of wind power generation forecast into power system operation, dispatch, and unit commitment procedures,” *IEEE Transactions on Sustainable Energy*, vol. 2, no. 4, pp. 433–442, Oct 2011.

[59] B. Lu and M. Shahidehpour, “Short-term scheduling of battery in a grid-connected PV/battery system,” *Power Systems, IEEE Transactions on*, vol. 20, no. 2, pp. 1053–1061, May 2005.

[60] M. Wang and H. Gooi, “Spinning reserve estimation in microgrids,” *Power Systems, IEEE Transactions on*, vol. 26, no. 3, pp. 1164–1174, Aug 2011.

[61] K. Rudion, A. Orths, Z. Styczynski, and K. Strunz, “Design of benchmark of medium voltage distribution network for investigation of DG integration,” in *Power Engineering Society General Meeting, 2006. IEEE*, 2006, pp. 1–6.

[62] D. Olivares, C. Canizares, and M. Kazerani, “A centralized energy management system for isolated microgrids,” *IEEE Trans. Smart Grid*, vol. 5, no. 4, pp. 1864–1875, July 2014.

[63] General motors corporation, my chevy volt website. [Online]. Available: http://www.mychevroletvolt.com.

[64] Time of Use (TOU) price in Ontraio, Ontraio Hydro Rates. [Online]. Available: http://www.ontario-hydro.com/index.php?page=current_rates.

[65] A. Mantawy, “A genetic algorithm solution to a new fuzzy unit commitment model,” *Electric Power Systems Research*, vol. 72, no. 2, pp. 171 – 178, 2004. [Online]. Available: http://www.sciencedirect.com/science/article/pii/S0378779604001087

[66] C.-C. Su and Y.-Y. Hsu, “Fuzzy dynamic programming: an application to unit commitment,” *Power Systems, IEEE Transactions on*, vol. 6, no. 3, pp. 1231–1237, Aug 1991.

[67] Gams development corporation, general algebraic modeling system (GAMS), software. [Online]. Available: http://www.gams.com.